Development of Pteropine Orthoreovirus Infection Mouse Model and its Application for the Evaluation of Therapeutics and Preventive Measures

（プテロパインオルソレオウイルス感染マウスモデルの開発とその治療・予防法の評価への応用）

2017

The United Graduate School of Veterinary Sciences,

Gifu University

(Gifu University)

EGAWA, Kazutaka

Development of Pteropine Orthoreovirus Infection Mouse Model and its Application for the Evaluation of Therapeutics and Preventive Measures

（プテロパインオルソレオウイルス感染マウスモデルの開発と
その治療・予防法の評価への応用）

EGAWA, Kazutaka

CONTENTS

PREFACE

Pteropine orthoreovirus (PRV), Nelson Bay strain (NB), was originally isolated from the heart blood of a grey-headed flying fox (*Pteropus poliocephalus*) in the Nelson Bay area of New South Wales in Australia in 1968 (25,26) and was classified into a member of the genus *Orthoreovirus* in the family *Reoviridae*.

Reoviruses (respiratory enteric orphan viruses), members of the family *Reoviridae*, are a relatively large and diverse group of non-enveloped virus with segmented double stranded RNA genomes (dsRNA) (65). The 15 genera of the *Reoviridae* are divided into 2 groups, *Sedoreoviridae* and *Spinareoviridae*. The subfamily *Sedoreoviridae*, which is almost spherical in appearance, comprises 6 genera, *Cardoreovirus*, *Miomoreovirus*, *Orbivirus*, *Phytoreovirus*, *Rotavirus*, and *Seadornavirus*. In contrast, the subfamily *Spinareoviridae*, which has large "spikes" or "turrets" at the 12 icosahedral vertices of the virus or core particle, comprises 9 genera, *Aquareovirus*, *Coltivirus*, *Cypovirus*, *Dinovernavirus*, *Fijivirus*, *Idonareovirus*, *Mycoreovirus*, *Oryzoreovirus*, and *Orthoreovirus*. The genus *Orthoreovirus* is divided into 2 subgroups based on the ability of the virus to induce cell-to-cell fusion and syncytium (21). One group is a fusogenic virus including avian orthreovirus (36), baboon orthoreovirus (BRV), reptilian orthoreovirus, broome reovirus (BroV), and PRV, and another group is a non-fusogenic virus including the prototypical mammalian orthoreovirus (MRV) (21,22,64).

The size of PRV is an approximately 80 nm in diameter. PRV has 2 protein shells with core spikes at the icosahedral vertices. PRV contains 10-segmented dsRNA divided into three classes based on their size: large (L1-L3), medium (M1-M3), and small (S1-S4). Each gene segment, except for S1 gene segment, is a monocistronic gene segment and produces each

protein, whereas S1 segment is a polycistronic gene segment and produces 3 proteins. L1, L2, L3, M1, M2, S1, S2, and S4 gene segments encode guanylyltransferase, RNA dependent RNA polymerase, major inner-capsid protein, minor inner-capsid protein, major outer-capsid protein, cell attachment protein, inner-capsid protein, and outer-capsid protein, respectively. The guanylyltransferase (L1), major outer-capsid protein (M2), cell attachment protein (S1), and outer-capsid protein (S4) are located on the surface of virions (19,63) and these proteins, except for major outer-capsid protein (M2), could be the targets of neutralizing antibodies (63,71). The cell attachment protein (S1), which probably forms a part of the viral minor outer capsid protein and is considered essential for virus infection, was also reported as a significant factor in pathogenesis (32). M3, S1, S1, and S3 gene segments encode μ NS, p10, p17, and σ NS, respectively. These viral proteins are non-structural proteins. The MRV μ NS and σ NS proteins are major constituent of cytoplasmic inclusion bodies (3,5,7). The p10 protein is a fusion-associated small transmembrane protein that has been shown to induce cell-to-cell fusion and the syncytium-inducing properties of fusogenic orthoreoviruses (56). The function of PRV p17 protein remains unclear, whereas ARV p17 protein is a CRM-1-independent nucleocytoplasmic shuttling protein, which plays a role in the nuclear process comprising gene transcription and cell growth regulation (54).

Reservoir of the genus *Orthoreovirus* is different at each species, and PRV is a potentially bat-originated virus. Fourteen PRV strains were isolated from fruit bats in Australia, Malaysia, PR China, and the Philippines between 1968 and 2017 (Table 1) (26,30,38,50,63). Indonesia/2010 strain was isolated from the salivary swab of *Pteropus vampyrus* imported to Italy from Indonesia in 2010 (20). PRV-neutralizing antibodies were detected in 83% of fruit bat species, *Rousettus amplexicaudatus*, *Eonycteris spelaea*, and *Macroglossus minimus*, in the Philippines, suggesting that PRV is generally prevalent in some species of wild bats in Southeast Asia (63).

Non-fusogenic MRVs are commonly prevalent and generally cause asymptomatic infection in humans. On the other hand, fusogenic orthoreoviruses sometimes cause severe diseases in animals, whereas the pathogenicity of those in humans has not yet been reported.

Melaka virus, a member of PRV, was isolated from a patient with acute respiratory tract infection (RTI) in Malaysia in 2006 (11). Three patients with PRV infection were reported in Malaysia in 2006 and 2010 (11-13). Four cases of PRV infection were identified as the imported cases from Indonesia to Japan and Hong Kong in 2007, 2009, and 2010 (10,68,69). Seven patients with influenza-like illness, such as fever, cough, and sore throat, caused by the infection with PRV, had been reported between 2006 and 2017 (Table 2) (10-13,68,69), indicating that PRV causes respiratory diseases in humans (10-13,68,69). However, the virulence of PRV in humans has not been elucidated fully. Animal models are required for the study on the elucidation of pathogenesis and for the evaluation of the drugs and vaccines developed for PRV infection. However, the PRV infection animal models have not yet been reported to date.

In Chapter 1, virulence, pathology and pathogenesis of human-borne PRV, which was isolated from a patient returned to Japan from Indonesia in 2007, and those of bat-borne PRV, which was isolated from a fruit bat in the Philippines in 2013, were elucidated in BALB/c mice. Fifty % lethal dose (LD_{50}) of the PRVs for the mice was determined. Viral loads in each organ were quantified by the quantitative RT-PCR and virus isolation method. Furthermore, the lesions in the mice were histopathologically and immunohistochemically analyzed.

In Chapter 2, immune response induced by infection with human-borne PRV was investigated in BALB/c mice. Therapeutic efficacy of antiserum with human-borne PRV-specific neutralizing antibody was also examined in BALB/c mice with lethal human-borne PRV infection. The study was carried out for investigation of a possibility of

vaccination and a usefulness of the neutralizing antibody as therapeutic agent for PRV infection.

In Chapter 3, a screening with use of a chemical library for therapeutic candidates against PRV infection was performed and ribavirin was identified as a therapeutic candidate. The therapeutic efficacy of ribavirin was also evaluated in BALB/c mice with lethal PRV infection.

Table 1. List of known strains of bat-borne PRV

No.	Name of isolate	Isolation year	Location of isolation (origin)	*Species of bat/specimens of isolation*	Reference
1	Nelson Bay	1968	New South Wales/Australia	*Pteropus poliocephalus/heart blood*	(26)
2	Pulau virus	1999	Tioman island/Malaysia	*Pteropus hypomelanus/urine*	(50)
3	Xi River	2010	Guangdong/PR China	*Rousettus leschenaultia/lung*	(20)
4	Indonesia/2010	2010	Italy (Indonesia)	*Pteropus vampyrus/salivary swab*	(38)
5	Cangyuan	2014	Yunnan/PR China	*Rousettus leschenaultia/intestinal content*	(30)
6	Samal-24	2017	Samal island/Philippines	*Eonycteris spelaea/throat swab*	(63)
7	Samal-50	2017	Samal island/Philippines	*Rousettus amplexicaudatus/throat swab*	(63)
8	Talikud-73	2017	Talikud island/Philippines	*Eonycteris spelaea/throat swab*	(63)
9	Talikud-74	2017	Talikud island/Philippines	*Eonycteris spelaea/throat swab*	(63)
10	Talikud-79	2017	Talikud island/Philippines	*Rousettus amplexicaudatus/throat swab*	(63)
11	Talikud-80	2017	Talikud island/Philippines	*Rousettus amplexicaudatus/throat swab*	(63)
12	Talikud-81	2017	Talikud island/Philippines	*Eonycteris spelaea/throat swab*	(63)
13	Talikud-82	2017	Talikud island/Philippines	*Rousettus amplexicaudatus/throat swab*	(63)
14	Talikud-83	2017	Talikud island/Philippines	*Eonycteris spelaea/throat swab*	(63)

Table 2. List of known strains of human-borne PRV

No.	Name of isolate	Isolation year and month	Location of isolation (origin)	Patient characteristics/ Specimens of isolation	Onset period/ Symptoms	Reference
1	Melaka	2006.03	Melaka, Malaysia	39-year-old man / Throat swab	4 days/ Fever (39.0°C), cough, sore throat, headache, myalgia, malaise, loss of appetite, generalized body weakness, prostration	(11)
2	Kamper	2006.08	Kamper, Malaysia	54-year-old man/ Throat swab	5 days/ Fever (40.1°C), cough, sore throat, headache, myalgia, malaise, loss of appetite, rigor, chills, body ache, nausea, vomiting, diarrhea, abdominal pain, generalized body erythema (face and upper trunk), conjunctivitis	(12)
3	HK23629/07	2007.04	Hong Kong (Bali, Indonesia)	51-year-old man/ Nasopharnygeal swab	A few days/ Fever (39.0°C), sore throat, myalgia, watery diarrhea	(10,68)

No.	Name of isolate	Isolation year and month	Location of isolation (origin)	Patient characteristics/ Specimens of isolation	Onset period/ Symptoms	Reference
4	Miyazaki-Bali/ 2007	2007.11	Miyazaki, Japan (Bali, Indonesia)	38-year-old man/ Throat swab	11 days/ Fever, cough, sore throat, joint pain	(69)
5	HK46886/09	2009.07	Hong Kong (Bali, Indonesia)	26-year-old woman/ Throat and nasal swab	Not described/ Influenza like illness	(68)
6	Sikamat	2010.03	Sikamat, Malaysia	46-year-old man/ Throat swab	6 days/ Fever (39.8°C), sore throat, headache, myalgia, malaise, loss of appetite, generalized body weakness, photophobia, abdominal pain, lethargy, erythematous flushing (face and chest), conjunctivitis	(13)
7	HK50842/10	2010.06	Not described (Indonesia)	29-year-old woman/ Throat and nasal swab	Not described/ Influenza like illness	(68)

CHAPTER 1

Virulence, Pathology and Pathogenesis of Human-borne Pteropine Orthoreovirus (PRV) and Bat-borne PRV in BALB/c Mice

Summary

Cases of respiratory tract infection (RTI) in humans due to Pteropine orthoreovirus (PRV) have been reported as an emerging virus infection in Southeast Asia. PRVs were isolated from patients with RTI and fruit bats in Southeast Asia, whereas the clinical course of PRV infections in humans is not elucidated fully. The virulence, pathology, and pathogenesis of two PRV strains, a PRV strain, which was isolated from a patient who imported it to Japan from Bali, Indonesia in 2007, and a bat-borne PRV, which was isolated from a bat (*Eonycteris spelaea*) in the Philippines in 2013, were investigated in BALB/c mice using virological and pathological methods. The intranasal inoculation of BALB/c mice with the PRV isolated from the patient with RTI caused RTI. Both PRV strains caused lethal respiratory disease in BALB/c mice. The pathogenicity of the bat-borne PRV was similar to those of the human-borne PRV in BALB/c mice. It was indicated that the BALB/c mice can be used for development of the animal model for PRV infection. The mouse model may help accelerating research on PRV.

Introduction

The presence of patients with respiratory tract infection (RTI) caused by infection with Pteropine orthoreovirus (PRV) in Southeast Asia suggests that PRV is a causative viral pathogen for RTI in humans. Some patients with PRV infection also showed the symptoms of abdominal pain, watery diarrhea, and vomiting (10,12,13,60). The possible cases of bat-to-human and human-to-human transmissions were reported (11-13,69). However, there is no evidence for the direct human-to-human or bat-to-human transmission of PRV. The disease spectrum and the pathogenesis of PRV infection in humans remain unclear. A new bat-borne PRV strain, which has high amino acid identities with a PRV isolated from a patient with RTI, who came back to Japan from Bali, Indonesia in 2007, was isolated from a bat (*Eonycteris spelaea, E. spelaea*) in the Philippines in 2013. It is still unknown whether PRV causes illnesses in fruit bats (60), whereas the bat-borne PRV is a potentially pathogenic to humans. Therefore, it is required to characterize both the PRV isolated from a patient and the bat-borne PRV isolated from fruit bat.

The PRV strain isolated from the above-mentioned Japanese man in 2007 was found to be lethal in C3H mice, but the virulence and pathology of this strain in the mice were not investigated in detail (32). As a common mouse model of respiratory syncytial virus (34) and influenza virus (70), which cause RTI in humans, BALB/c mouse may be a feasible animal model for PRV infection. BALB/c mouse, which is widely used to prepare the monoclonal antibody, is also broadly used in immunological research, especially in vaccine testing of hepatitis C virus (1), severe acute respiratory syndrome coronavirus (61), Middle East respiratory syndrome coronavirus (33), and so on. In this Chapter, the virulence of the PRV isolated from human, and pathology and pathogenesis of the PRV infection were elucidated in BALB/c mouse. The pathogenicity (virulence, pathology, and pathogenesis) of the

bat-borne PRV was also examined in BALB/c mice and was compared with that of PRV human isolate. An animal model for PRV infection was developed using BALB/c mouse.

Materials and Methods

Viruses and cells

A PRV strain Miyazaki-Bali/2007 (PRV-MB), which was isolated in the previous studies, was used (69). The PRV strain was isolated from a patient with RTI, who came back to Japan from Bali, Indonesia, in 2007 (59,69). The nucleotide sequence of 10 segments are deposited in GenBank under the accession numbers; AB908278, AB908279, AB908280, AB908281, AB908282, AB908283, AB908284, AB908285, AB908286, and AB908287. A PRV strain Samal-24 (PRV-Samal-24) was isolated from *E. spelaea* in the Philippines in 2013 (61). The nucleotide sequence of the 10 segments are also deposited in GenBank under the accession numbers; LC110198, LC110199, LC110200, LC110201, LC110202, LC110203, LC110204, LC110205, LC110206, and LC110207.

PRVs were propagated in human embryonic kidney-derived 293FT cells (Thermo Fisher Scientific, Inc.) for the preparation of the working virus solution. Cells infected with PRV-MB were cultured at 37°C in Dulbecco's modified eagle's medium (DMEM; Sigma-Aldrich Co., LLC) supplemented with 5% heat-inactivated fetal bovine serum (FBS) and 1% antibiotics (penicillin and streptomycin; Pen-Strep, Thermo Fisher Scientific, Inc.) (DMEM-5FBS). After 2 days of culture, the medium was centrifuged at 800 × *g* for 5 min to remove cellular debris. The supernatant was overlaid onto 20% sucrose in a 50 mL tube (Becton Dickinson, Ltd.) and centrifuged at 100,000 × *g* for 2 h to concentrate the virus. The concentrated virus was dissolved with DMEM with 2% FBS and 1% Pen-Strep (DMEM-2FBS), and the aliquots were stored at -80°C until use.

Determination of infectious dose of PRV with a plaque assay

The infectious dose of each strain was determined in a plaque assay in Vero cell (ATCC,

CCL-81) monolayers as described previously (69). The cells were inoculated with serially diluted virus solution of PRV-MB or PRV-Samal-24 and incubated for 1 h at 37°C for adsorption. The cell monolayers were washed with phosphate buffered saline solution (PBS), and the cells were cultured with DMEM-5FBS supplemented with 0.8% agarose for 2 days at 37°C. Plaque was visualized by staining the cells with neutral red solution. Plaques were counted, and the virus titers were calculated in plaque forming units per milliliter (PFU/ml).

Mice

Nine-week-old female BALB/c mice (Japan SLC, Inc.) were used. The mice used were healthy and weighed approximately 20 g.

Determination of 50% lethal dose for PRV-MB

The mice, which were anesthetized with a combination of ketamine (100 mg/kg) and xylazine (4 mg/kg) in 0.9% sodium chloride solution, were inoculated with each strain of PRV. The mice (5 per group) were intranasally inoculated with 1.0×10^3 to 1.0×10^6 PFU of each PRV strain in 20 μL DMEM-2FBS. The clinical signs and body weight of the mice were monitored for 14 days and the 50% lethal dose (LD_{50}) of PRV was calculated according to the method of Reed and Muench (52). Mice that were intranasally inoculated with 20 μL DMEM-2FBS without PRV were used as the control. The changes in body weight and the survival rates were plotted using the GraphPad Prism software program (GraphPad Software, Inc.) and were statistically analyzed by a one-way ANOVA.

Quantitative detection of the PRV genome in organs and blood

Five mice were intranasally inoculated with 1.0×10^5 PFU of PRV-MB or PRV-Samal-24 strain as described above. The mice were sacrificed on the 5th or 6th day

post-infection (DPI), and then blood and the organs (the head including the brain and the nasal cavity, trachea, lung, liver, kidney, spleen, and intestine) were collected. The viral RNA load in each organ and blood was determined by a quantitative real-time RT-PCR (qRT-PCR) as described below.

Determination of viral RNA load with a quantitative real-time RT-PCR

Blood samples were collected from the mice (5 per group) infected with each strain of PRV by cardiac puncture. Each of the blood samples was mixed with Isogen LS (Wako Pure Chemical Industries, Ltd.), and total RNA was extracted from each blood sample according to the manufacturer's instructions. The organs and tissues; the brain, nasal cavity, trachea, lung, heart, liver, spleen, kidney, and intestine were collected. These samples were immediately submerged in RNAlater (Ambion, Life Technologies, Inc.) and stored at -80°C until use. Total RNA was extracted using Isogen (Wako Pure Chemical Industries, Ltd.) according to the manufacturer's instructions. The viral copy numbers were determined with a qRT-PCR as follows. The forward and reverse primers, and probe were specifically designed according to the nucleotide sequence of the outer-capsid protein (OCP) region in the S4 segment of PRV-MB or to that of PRV-Samal-24. The sequences of the forward primer, the reverse primer, and the probe for the amplification of the PRV-MB genome were 5'-CATTGTCACTCCGATCATGG-3', 5'-TGGGAGTGTGCAGAGCATAG-3' (Eurofins Genomics, Inc.), and FAM/5'-GTAGGTATGCCACTCGTGGAATCC-3'/TAMRA (Sigma-Aldrich Co. LLC.), respectively. The sequences of the forward primer, the reverse primer, and the probe for the amplification of the PRV-Samal-24 genome were 5'-CAATTTCCACTCGTTCGTTG-3', 5'- GATGGTGTGGAAACGGATAC -3' (Eurofins Genomics, Inc.), and FAM/5'- GACCAGACCAGATACGTGGAATCC -3'/TAMRA (Sigma-Aldrich Co. LLC.), respectively. The qRT-PCR was performed using a Light Cycler

96 system (Roche Diagnostics, Ltd.) with a QuantiTect Probe RT-PCR Kit (Qiagen, Ltd.). The Light Cycler experimental protocol was as follows: reverse transcription (50°C for 30 min), denaturation (95°C for 15 min), and 45 cycles of amplification and quantification (94°C for 15 s and 60°C for 60 s), followed by a final cooling step at 40°C for 30 s. In this study, the standard controls for PRV-MB and PRV-Samal-24 were 10-fold serial dilutions of the plasmid DNA containing the S4 segments of PRV-MB and PRV-Samal-24, respectively. The viral copy numbers in the samples were calculated as the ratio of the copy numbers of each standard control. The viral copy numbers were plotted using the GraphPad Prism software program and the results were statistically analyzed by a one-way ANOVA. The viral RNA detection limits in the blood, trachea, and the other tissues were determined to be 2.5×10^3 copies/ml, 1.6×10^3 - 5.0×10^3 copies/0.1g, and 2.5×10^3 copies/0.1g, respectively. One PFU was equivalent to 2.9 copies of viral RNA.

Quantitative of the infectious PRV in the organs

Two mice were intranasally inoculated with 1.0×10^6 PFU of the PRV-MB strain or of PRV-Samal-24 strain as described above. The mice were sacrificed on the 4th DPI, and organs (the head including the brain and the nasal cavity, trachea, lung, liver, kidney, and intestine) of the mice were collected. The infectious virus titer in each organ was determined by a plaque assay as described below. Each organ collected was immediately submerged in DMEM-2FBS and homogenized and centrifuged at 800 × *g* for 5 min to remove debris. The supernatant fraction was collected and stored at -80°C until use. The virus titer in the supernatant fraction was determined in a plaque assay in Vero cell monolayers as described previously (69). The virus titers were plotted using the GraphPad Prism software program. The virus titer detection limit was determined to be 2.4×10^1 PFU/0.1 g.

Time-course analysis in the lung of mice infected with PRV

The mice intranasally infected with 1.0×10^3 PFU of PRV-MB (PRV-MB-1.0×10^3 PFU mice) and the mice intranasally infected with 1.0×10^5 PFU of PRV-MB (PRV-MB-1.0×10^5 PFU mice) were sacrificed by exposure to excess isoflurane, and the lungs were collected on the 1st, 3rd, and 5th DPI. The virus RNA loads in the lungs was determined with the qRT-PCR. The viral copy numbers were plotted using the GraphPad Prism software program and the results were statistically analyzed by a one-way ANOVA. The lungs were examined for pathological analyses with the immunohistochemical (IHC) analysis as described below.

Histopathology and immunohistochemistry

The collected tissues were stained with hematoxylin and eosin (H&E) for histopathology. An IHC analysis was performed for the detection of PRV antigen in the tissues. The IHC analysis methods were the same as those described previously except for the antigen detection antibody (35). The sections were deparaffinized by placing them in a retrieval solution (pH 6) (Nichirei Biosciences, Inc.), followed by heat-treatment in an autoclave at 121°C for 10 min. The polyclonal antibody to the OCP (S4 segment) of PRV-MB raised in a rabbit by immunization with the antigen (OCP antibody) was used for the IHC detection of PRV antigen (57). To validate whether the OCP antibody reacted with the mouse lungs non-specifically, the lung tissues of 6-month-old BALB/c mice infected with severe acute respiratory syndrome coronavirus (SARS-mouse-lung), in which severe inflammation was shown, and those of the mice inoculated with mock solution (mock-mouse-lung) (42) were tested with IHC analysis. The SARS-mouse-lung (left panels) and mock-mouse-lung were stained with the OCP antibody in the IHC to determine whether the positive OCP antibody reaction in IHC was specific to PRV or not. The samples showed a negative reaction in the IHC analysis (Figure 1), indicating that the OCP antibody did not react non-specifically with

the mouse lungs with inflammation and that the positive signals detected in the IHC analysis indicate the presence of the OCP of PRV (Figure 1). As the negative control, normal rabbit serum (NRS; Dako, Ltd.) was used in IHC analysis. After treatment, the sections were reacted with the OCP antibody or NRS and then washed with PBS. The sections were incubated with Nichirei-Histofine Simple Stain Mouse MAX PO (R) (Nichirei Biosciences, Inc.) in accordance with the manufacturer's instructions. The peroxidase activity was detected with 3, 3'-diaminobenzidine (Sigma-Aldrich Co. LLC.), and the sections were counterstained with hematoxylin.

Ethics statement

The animal studies were carried out in strict accordance with the Guidelines for Proper Conduct of Animal Experiments of the Science Council of Japan and the strict compliance with animal husbandry and welfare regulations. All animal experiments were approved by the Committee on Experimental Animals at the National Institute of Infectious Diseases (NIID) in Japan (Approval No. 215016,116086, and 116082). All of the animals infected with PRV were handled in biosafety level 3 animal facilities, in accordance with the guidelines of the NIID. The mice were inoculated with virus solution under proper anesthesia, and all efforts were made to minimize the potential pain and distress. After inoculation, the animals were monitored once a day during the study period. The humane endpoint was introduced for all mice displaying >25% initial body weight loss.

Results

Symptoms and viral loads in BALB/c mice infected with PRV-MB

The PRV-MB-1.0×10^5 PFU mice or the PRV-MB-1.0×10^6 PFU mice developed symptoms (piloerection, slowness in movement, anorexia, and weight loss) from the 2nd DPI. All the mice died by the 6th DPI (Figure 2). The severity of the symptoms in the PRV-MB-1.0×10^4 PFU mice was less than that in the PRV-MB-1.0×10^5 PFU mice or the PRV-MB-1.0×10^6 PFU mice, and 3 of the 5 mice died by the 8th DPI. The extent of body weight loss in the PRV-MB-1.0×10^3 PFU mice was greater than that in the control mice. The PRV-MB-1.0×10^3 PFU mice did not show any symptoms other than body weight loss. The LD_{50} of PRV-MB in BALB/c mice was determined to be 6.8 × 10^3 PFU/head.

The level of viral RNA in the lungs (average level, 6.9 × 10^8 copies/0.1g) was higher than those in the other organs (Figure 3A, left panel). Viral RNA was detected in the blood (maximum level of 7.5 × 10^6 copies/ml) (Figure 3A, right panel). In contrast, viral RNA was not detected in the brain, heart, liver, spleen, kidney, and intestine. The infectious virus was detected only in respiratory organs (Figure 3B). The titer in the lungs (average virus titer, 6.4 × 10^4 PFU/0.1g) was the highest among the organs tested.

Pathology of the lower respiratory tract in BALB/c mice infected with PRV-MB

A pathological examination revealed tissue damage and inflammation (i.e. necrosis and the accumulation of inflammatory cells including lymphocytes) in the lower respiratory tract, including the bronchiole and alveoli, on the 4th DPI (Figure 4A, left and middle panels). Neutrophils and type II pneumocytes infiltrated to the alveoli and alveolar walls, and tissue

damage in the lungs was detected (Figure 4B). The PRV antigen-positive lesions revealed in the IHC analysis by using the OCP antibody showed negative reaction in the IHC analysis using NRS (Figure 4A, right panels). No pathological changes or viral antigens were detected in the other tissues examined.

Viral genome loads in the lungs according to the time course

The viral RNA in the lungs of the PRV-MB-1.0×10^3 PFU mice or the PRV-MB-1.0×10^5 PFU mice was determined throughout the course of infection (Figure 5). On the 1st DPI, the viral RNA load in the lungs of the PRV-MB-1.0×10^5 PFU mice was similar to that of the PRV-MB-1.0×10^3 PFU mice. In contrast, on the 3rd and 5th DPI, the viral RNA load in the lungs of the PRV-MB-1.0×10^5 PFU mice was significantly higher in comparison to the PRV-MB-1.0×10^3 PFU mice.

The presence of viral antigens in the lungs of the PRV-MB-1.0×10^3 PFU mice and the PRV-MB-1.0×10^5 PFU mice was investigated on the 1st, 3rd, and 5th DPI. Viral antigens were detected in the bronchial epithelium of the PRV-MB-1.0×10^5 PFU mice on the 1st DPI (Figure 6B, upper panel), in the alveolar duct and alveoli, and bronchial epithelium on the 3rd DPI, and in the alveolar area on the 5th DPI (Figure 6B, middle and lower panels). Cellular damage characterized by positive nuclear aggregation, cellular atrophy, and cellular debris was detected in the terminal bronchiole, which was also positive for PRV-MB antigen (Figure 7). PRV-MB caused extensive and massive pulmonary infection in the PRV-MB-1.0×10^5 PFU mice. In contrast, few viral antigens were detected in the bronchial epithelium of the PRV-MB-1.0×10^3 PFU mice on the 1st and 3rd DPI (Figure 6A, upper and middle panels, respectively), and no viral antigens were detected in the bronchial epithelium or alveoli on the 5th DPI (Figure 6A, lower panel).

Virulence and pathogenicity of PRV-Samal-24 in BALB/c mice

Nine-week-old BALB/c mice were infected with a graded dosage (1.0×10^3 - 1.0×10^6 PFU) of PRV-Samal-24. The intranasal inoculation of the mice with PRV-Samal-24 led to fatal outcomes. The LD_{50} of PRV-Samal-24 for BALB/c mice was determined to be 4.2×10^3 PFU/head (Figure 8).

Among the respiratory organs, viral RNA was detected in the lungs of the mice infected with PRV-Samal-24; the viral RNA copy numbers in the lungs were up to 3.7×10^8 copies/0.1g on average (Figure 9A, left panel). Viral RNA was also detected in the blood (maximum level, 1.8×10^6 copies/mL) (Figure 8A, right panel). In addition, the infectious virus was isolated from the lungs (Figure 9B). The infectious dose of PRV-Samal-24 was the highest in the lungs among the tissues tested with the dose being up to 9.5×10^3 PFU/0.1g on average.

Pathological examination of the PRV-Samal-24-1.0×10^6 PFU mice was revealed inflammatory lesions in the lungs (by H&E staining) (Figure 10, left panels), and viral antigens were detected, especially from the bronchiole to the alveoli (by IHC staining) (Figure 10, right panels) as was observed with PRV-MB infection in mice.

Discussion

The present study showed through virological and pathological examinations that the lung was the principle target organ of PRV replication after intranasal inoculation of BALB/c mice with PRV. PRV mainly replicated in the bronchiolar epithelium by the 3rd DPI. The bronchiolar epithelium is composed of ciliated cells and nonciliated cells, such as clara cells and goblet cells, which are classified as secretory cells (48). Morphologically, the PRV antigen-positive cells were likely to be clara cells and goblet cells. PRV infection caused severe inflammation in the lungs of the mice on the 4th DPI (acute phase). Morphologically, PRV mainly replicated in the pneumocyte-like cells were likely to be Type I pneumocytes, which are involved in the process of gas exchange between the alveoli and blood (28). Mammalian orthoreovirus, which is classified to the genus *Orthoreovirus* in the family *Reoviridae*, is reported to replicate in Type I pneumocytes, and has been shown to induce severe pneumonia in some rodent species, including mice and rats (27,41). Type I pneumocytes might be a critical replication site for PRV. It was assumed that fatal outcomes were induced in mice infected with a lethal dose of PRV due to a decrease in the respiratory function that occurred as a result of the destruction of the bronchiolar epithelial cells and pneumocytes. In this study, the cell types in which PRV replicated were identified only by morphological observation. Further studies are needed to elucidate the primary target cells, which are infected with PRV and in which PRV replicates. The high-titer PRV genome and infectious PRV were detected in the lungs of the mice infected with a lethal dose of PRV on the 4th to 6th DPI (acute phase) (Figure 3A). BALB/c mice were susceptible to PRV and developed RTIs, similarly to humans. Demonstration of infectious PRV in lungs indicates that PRV definitely replicated there (Figure 3B). Koch's postulates (i.e. isolation of PRV from patients with RTIs, induction of RTI in mice by infection with PRV, and detection of

infectious PRV in respiratory organs of mice infected with PRV) support a causal role of PRV infection in the development of respiratory diseases in humans (31).

The virulence, pathology and pathogenesis of PRV-Samal-24 were evaluated in BALB/c mouse model. Similarly to PRV-MB, PRV-Samal-24 caused viremia and respiratory disease in the BALB/c mice. The amino acid identities (encoded by each gene segment) between PRV-Samal-24 and PRV-MB were as follows (63): cell attachment protein region of the S1 segment, 82%; p10 region of the S1 segment, 100%; p17 region of the S1 segment, 94%; inner-capsid protein region of the S2 segment, 97%; σ NS region of the S3 segment, 97%; OCP region of the S4 segment, 97%; minor inner-capsid protein region of the M1 segment, 94%; major outer-capsid protein region of the M2 segment, 95%, μ NS region of the M3 segment, 91%, guanylyltransferase region of the L1 segment, 94%, RNA polymerase region of the L2 segment, 98%, and major inner-capsid protein region of the L3 segment, 98%. PRV-Samal-24 and PRV-MB were also reported to show cross-reactivity in an immunofluorescence assay (63). As both the *in vivo* and *in vitro* characteristics of PRV-Samal-24 are similar to PRV-MB, it is possible for PRV-Samal-24 to cause illness in humans.

In conclusion, a BALB/c mouse model of PRV infection, in which PRV caused RTI, was developed. Immunocompetent BALB/c mice were sensitive to PRV, when the mice were infected with PRV intranasally. This model may be useful for analyzing the virulence of PRV and pathogenicity of PRV infection in BALB/c mice. Furthermore, the model may be useful for evaluation of the efficacy of the drug and vaccines developed for PRV infections (See Chapter 2 and 3)

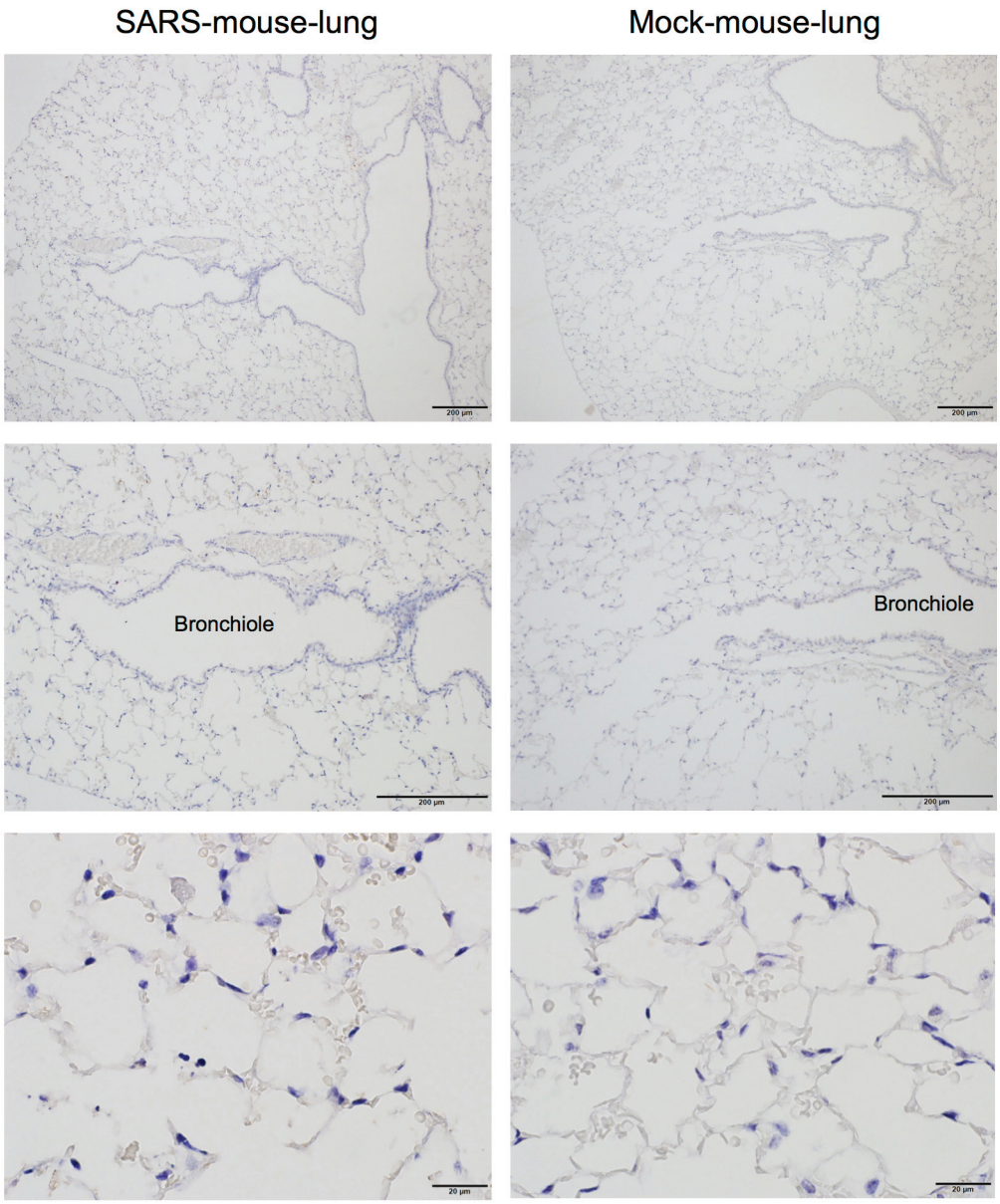

Figure 1. Validation of the specificity of the OCP antibody in the detection of PRV antigen in IHC

The SARS-mouse-lung (left panels) and mock-mouse-lung (right panels) (42) were examined by IHC with using the OCP antibody. The IHC signals in the lung at 100× magnification (upper panels), the bronchiole at 200× magnification (middle panels), and the alveolus at 1000×magnification (lower panels) are shown. No signal, which indicates non-specific reaction of the OCP antibody, was detected in the SARS-mouse-lung, in which

severe inflammation was found on H&E staining (42), and mock-mouse-tissue. The scale bars in upper and middle panels indicate 200 μm, whereas those in lower panels indicate 20 μm.

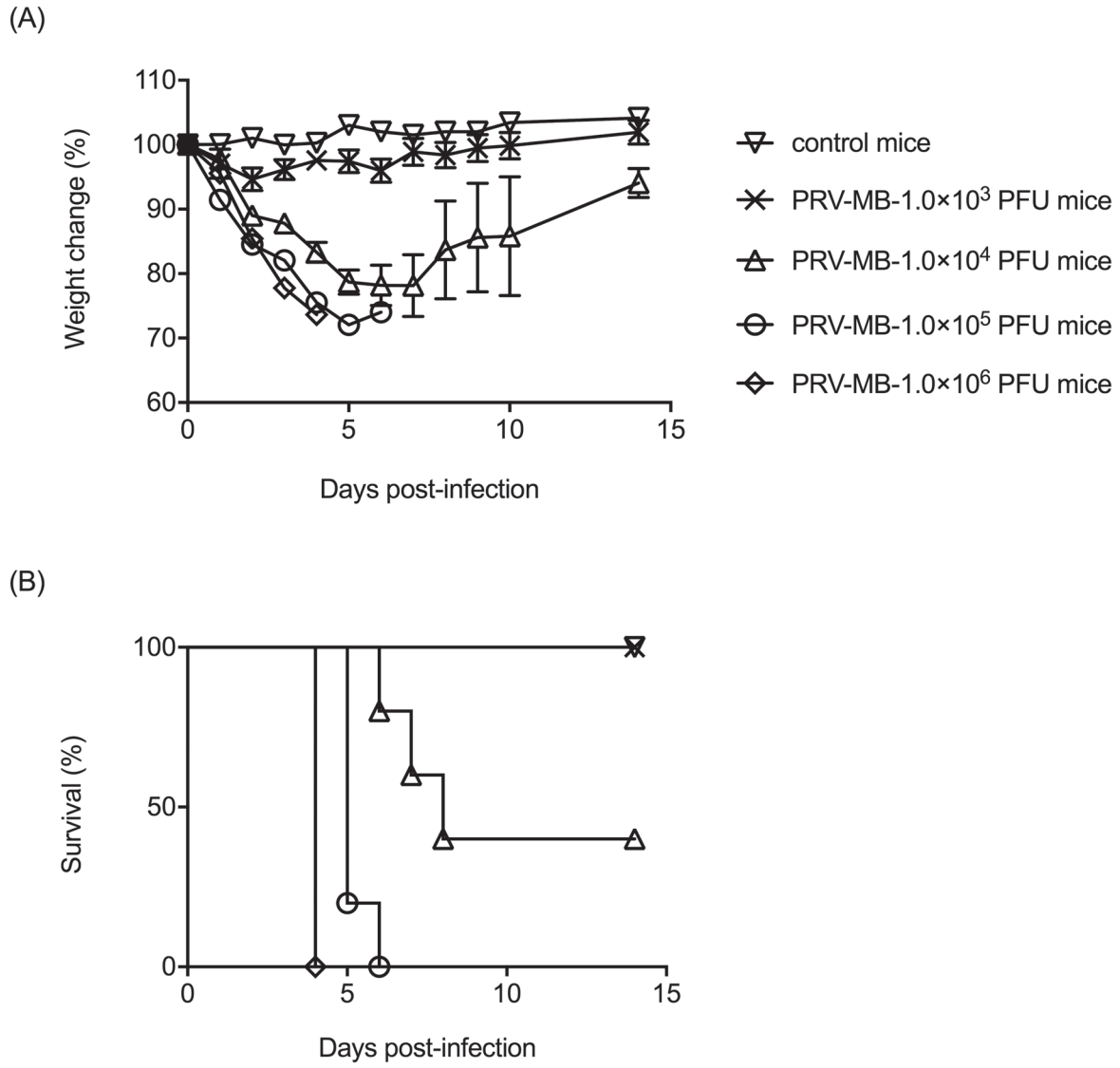

Figure 2. Changes in the body weight (A) and survival rate (B) of BALB/c mice intranasally inoculated with 1.0×10^3 - 1.0×10^6 PFU of PRV-MB and the control mice.

The mice infected with each dose of PRV-MB are shown (5 mice per group). Error bars in A indicate the standard error.

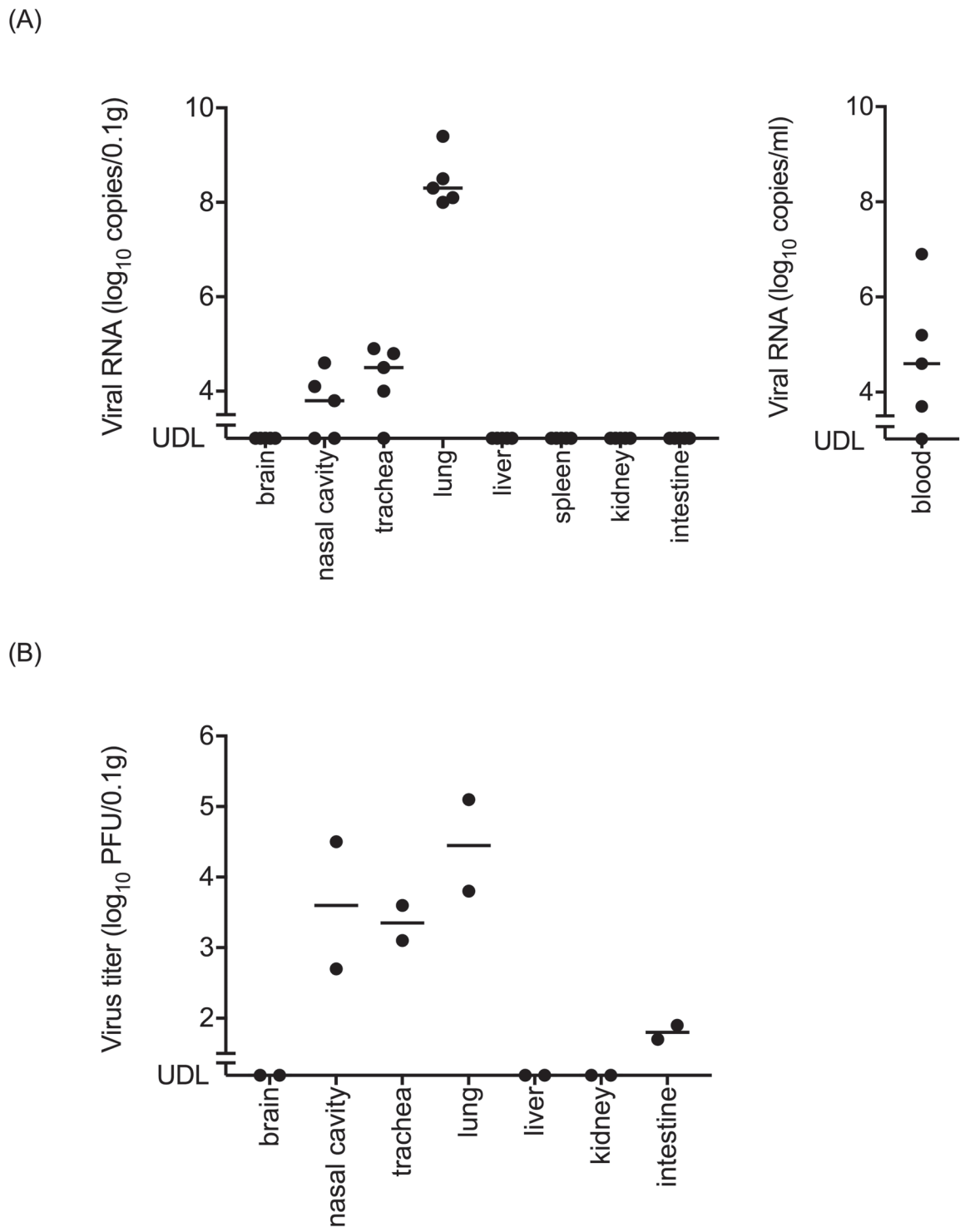

Figure 3. Viral RNA loads in each organ and the blood (A) and infectious virus titers in each organ (B) of BALB/c mice infected with PRV-MB.

(A) The organs and blood samples were obtained from the PRV-MB-1.0×10^5 PFU mice on the 5th or 6th DPI (5 mice per group). The left and right panels indicate the viral RNA

loads in the organs and blood of the mice, respectively. (B) The organs were obtained from the PRV-MB-1.0×10^6 PFU mice on the 4th DPI (2 mice per group). UDL, under detection limit.

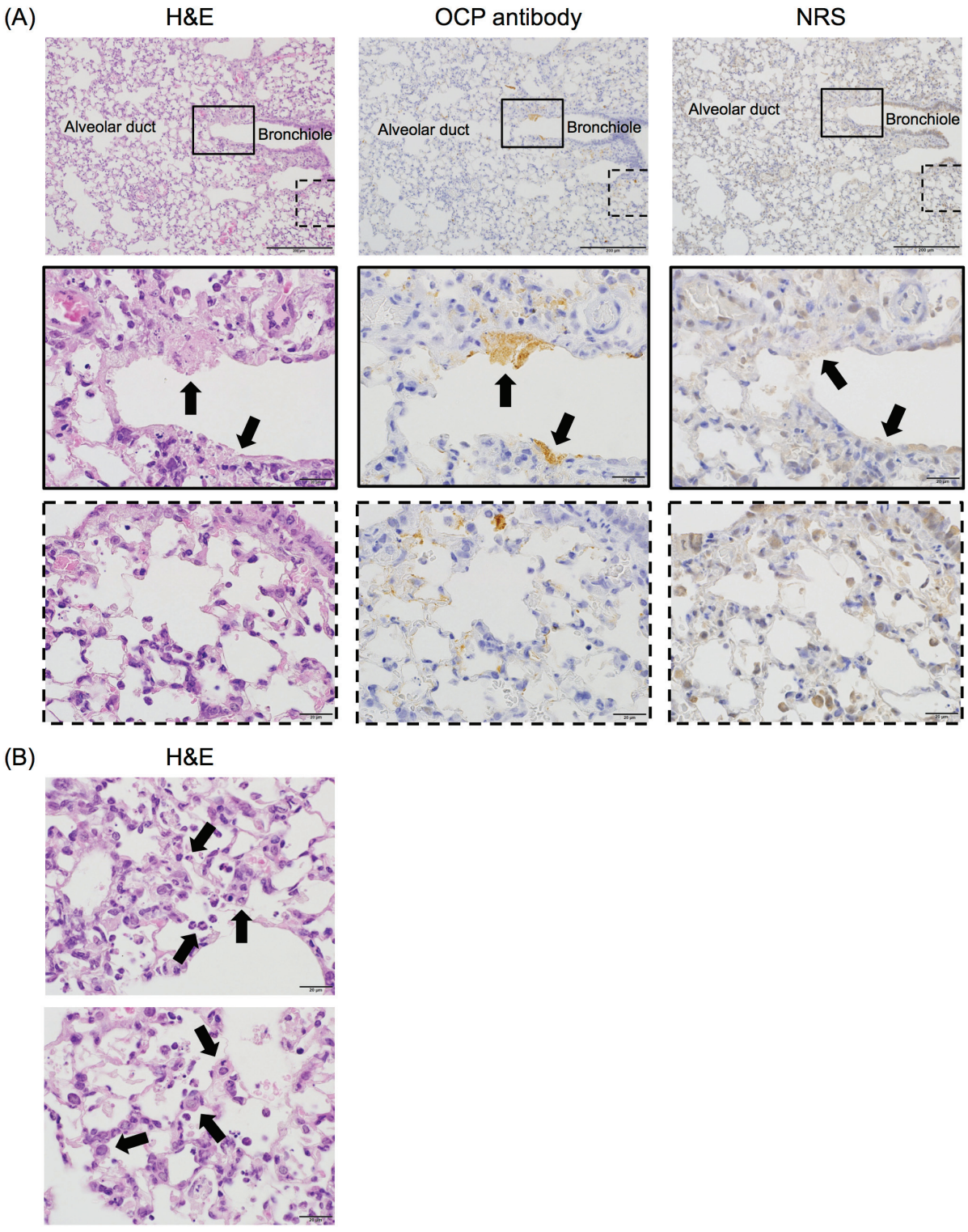

Figure 4. Histopathological findings of the lungs of BALB/c mice infected with PRV-MB.

The lungs were obtained from PRV-MB-1.0×10^6 PFU mice on the 4th DPI. H&E

staining (A, left panels, and B) and IHC analysis with an OCP antibody (A, middle panels) or with a NRS (A, right panels) were performed. The H&E staining and IHC with an OCP antibody or with NRS of the lung at 200× magnification (A, upper panels), of the bronchiole at 1000× magnification (A, middle panels), and of the alveolus at 1000× magnification (A, lower panels) are shown. The black boxes in the upper panels indicate the necrotic legion, which was positive for PRV-MB antigen (A, upper-middle panel). These areas are shown at higher magnification in the middle panels. The black arrows in the middle panels indicate the area of bronchiolar epithelial cell necrosis. The black dotted boxes in the lower panels indicate the PRV-MB antigen-positive lesion in the alveolar area (A, lower-middle panel). The PRV-MB antigen-positive lesion did not show a positive reaction in the IHC analysis, in which NRS was used instead of the OCP antibody (A, right panels). The scale bars in A (upper panels) indicate 200 μm, whereas those in A (middle panels), and A (lower panels) indicate 20 μm. H&E staining images of the alveoli at1000× magnification (B) are shown. The black arrows in the upper and lower panels indicate neutrophils and type II pneumocytes, respectively. The scale bars in (B) indicate 20 μm.

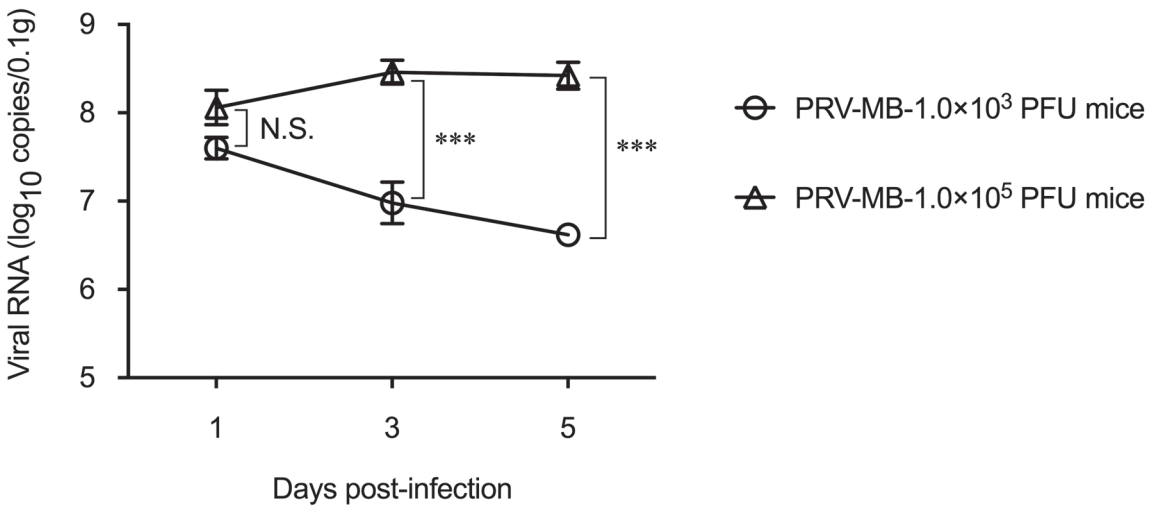

Figure 5. Temporal changes in the viral RNA loads in the lungs of the BALB/c mice infected with PRV-MB.

The lungs were obtained from the PRV-MB-1.0×10^3 mice or the PRV-MB-1.0×10^5 PFU mice on the 1st, 3rd, and 5th DPI (5 mice per group for each day). Error bars indicate the standard error. N.S., not significant. ***, statistically significant ($p < 0.0001$).

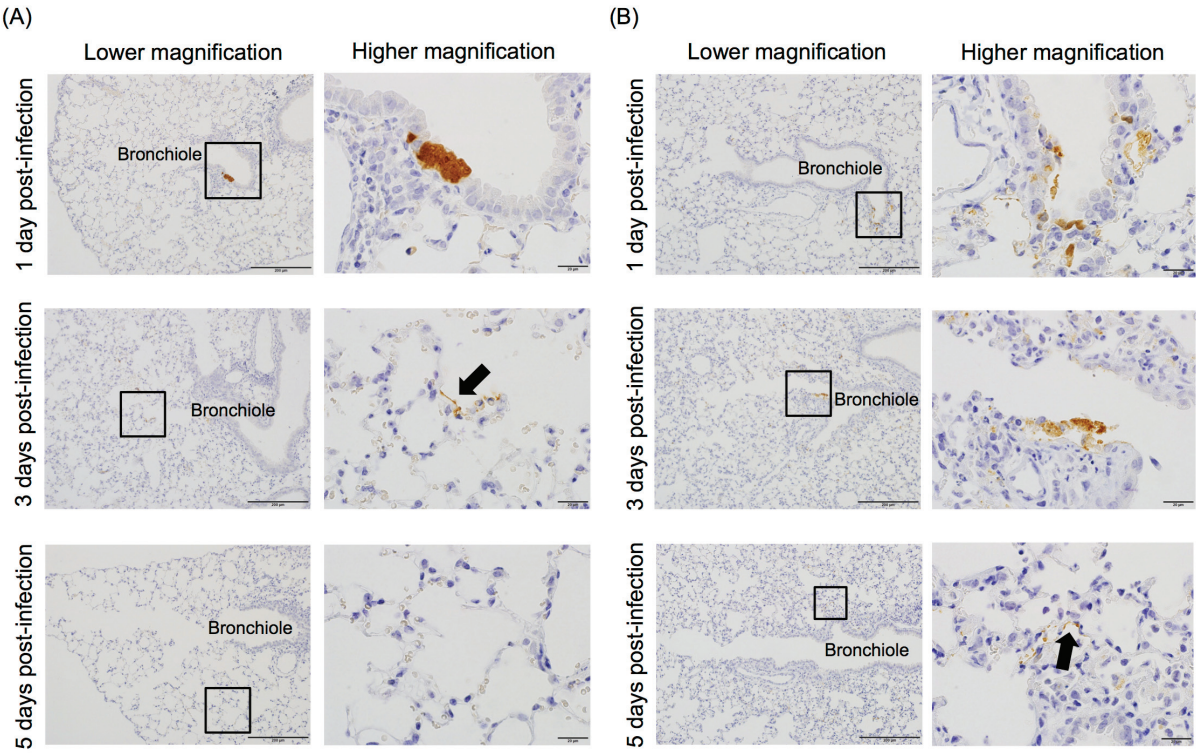

Figure 6. Histopathological findings in the lungs of BALB/c mice infected with PRV-MB on the 1st, 3rd, and 5th DPI.

The lungs were obtained from the PRV-MB-1.0×10^3 PFU mice (A) and the PRV-MB-1.0×10^5 PFU mice (B) on the 1st, 3rd, and 5th DPI. IHC analysis of the lungs was performed using the OCP antibody for detection of PRV antigen. The right panels show enlarged views of the areas of interesting lesions (black squares in the left panels). The magnification levels of the left and right panels are 200× and 1000×, respectively. Black arrows indicate the pneumocytes that were positive for PRV-MB antigen. The scale bars in the left and right panels indicate 200 μm and 20 μm, respectively.

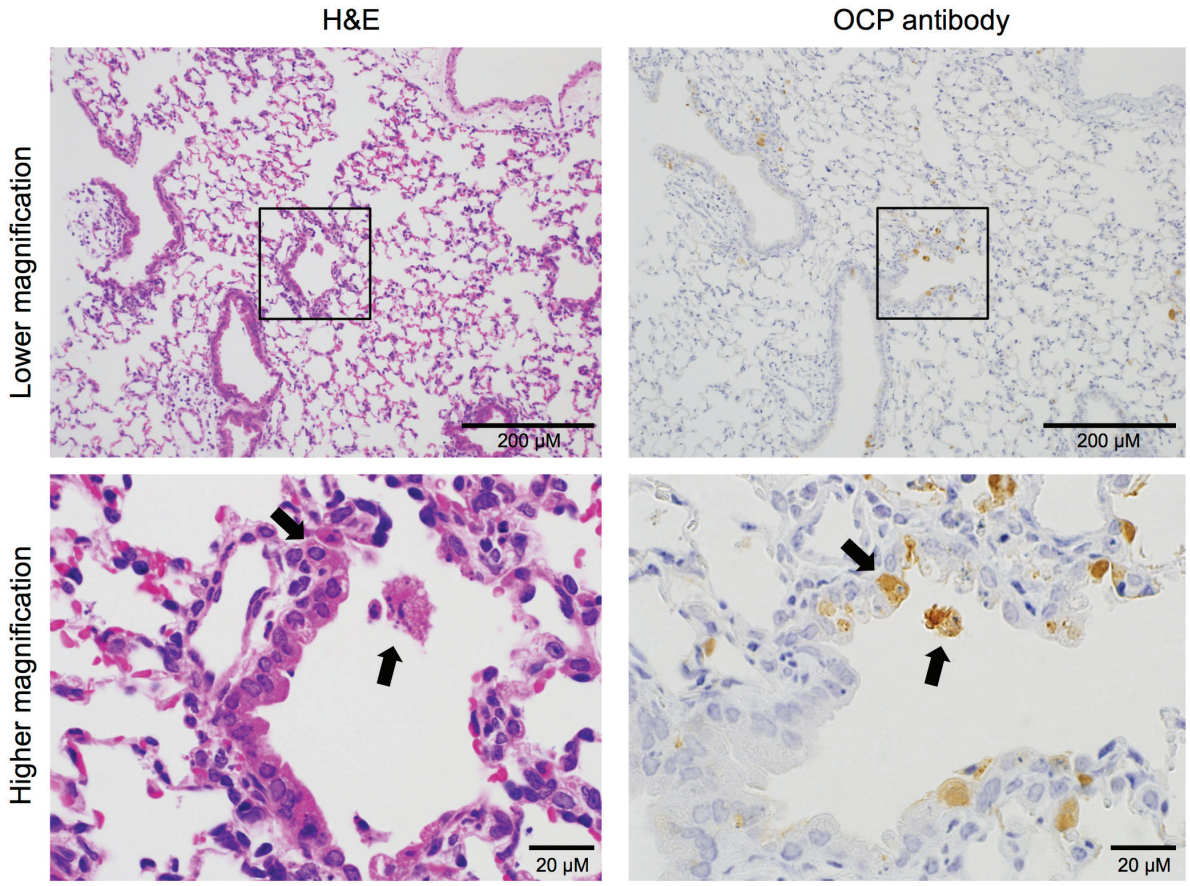

Figure 7. Histopathological findings in the terminal bronchiole of the BALB/c mice infected with a lethal dose of PRV-MB on the 1st DPI.

The lungs from the PRV-MB-1.0×10^5 PFU mice were obtained on the 1st DPI. The lungs were H&E stained (left panels) and tested immunohistochemically using the OSP antibody (right panels). The lower panels show enlarged views of the areas of interesting lesions (black squares in the upper panels). The black arrows indicate necrotic cells and cellular debris. The magnification levels of the upper and lower panels are 200× and 1000×, respectively. The scale bars in the upper and lower panels indicate 200 μm and 20 μm, respectively.

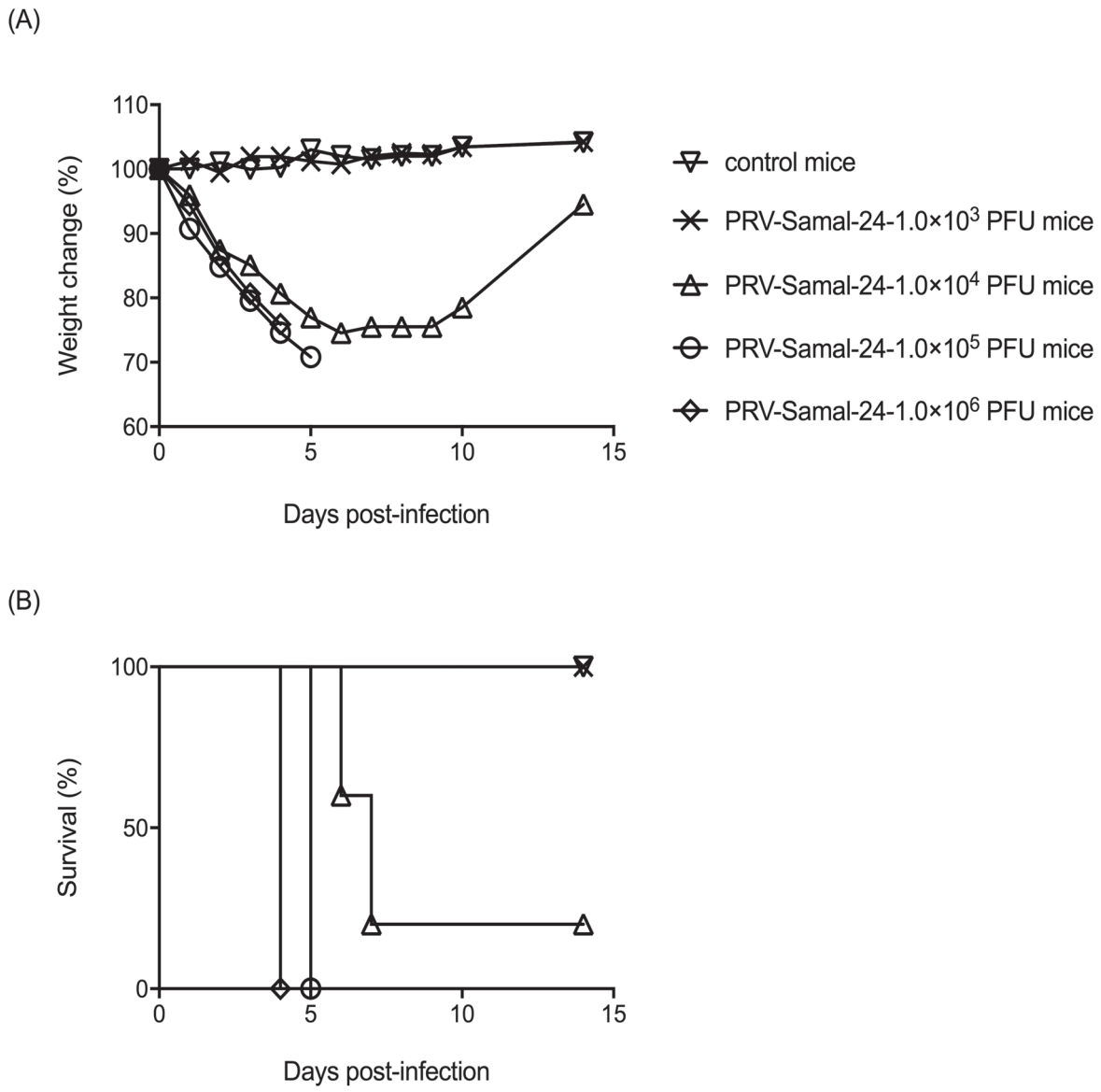

Figure 8. Changes in the body weight (A) and survival rate (B) of BALB/c mice intranasally inoculated with $1.0 \times 10^3 – 1.0 \times 10^6$ PFU of PRV-Samal-24 and the control mice.

The mice infected with each dose of PRV-Samal-24 are shown (5 mice per group). Error bars in A indicate the standard error.

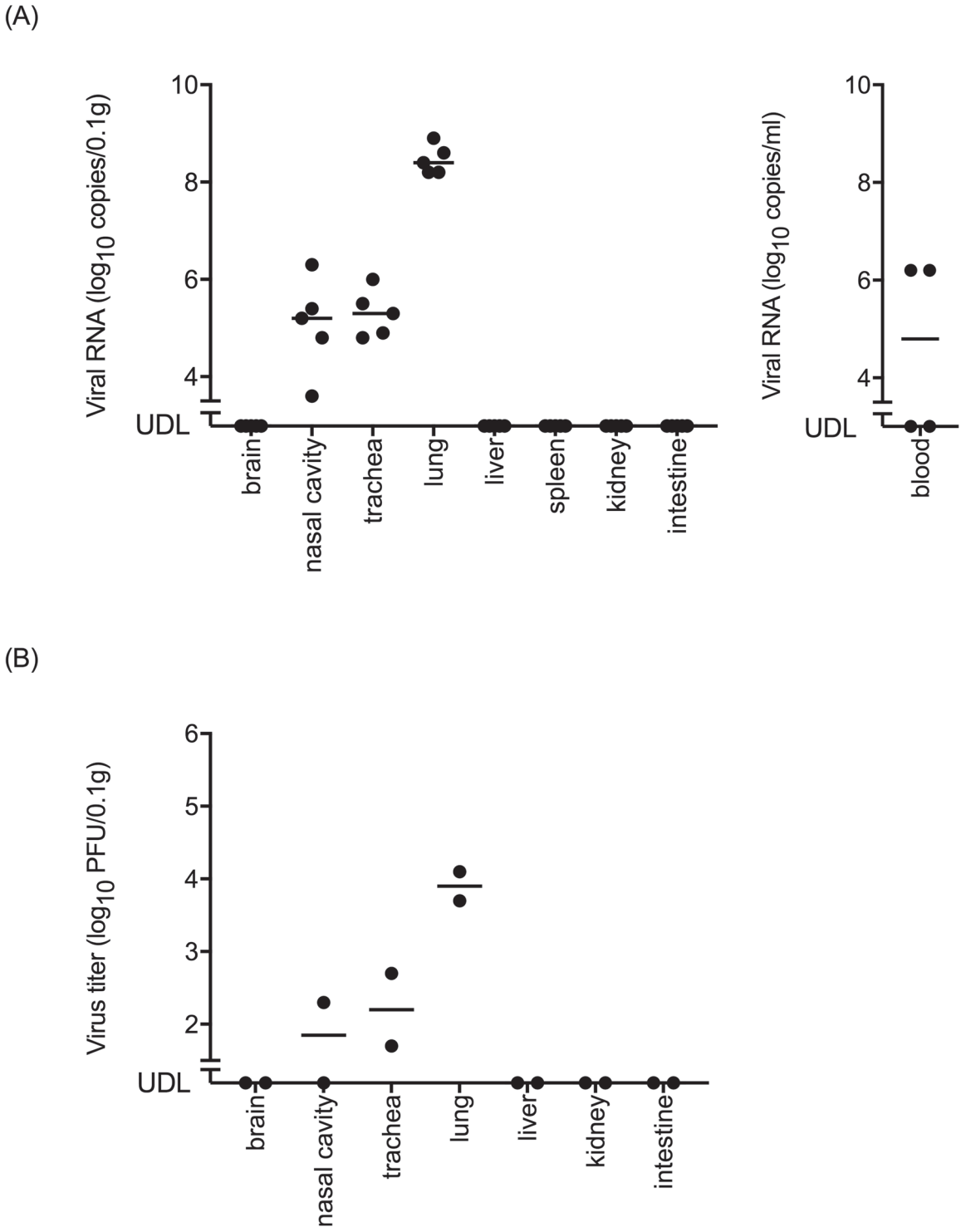

Figure 9. Viral RNA loads in each organ and the blood (A), and infectious virus titer in each organ (B) of BALB/c mice infected with PRV-Samal-24.

(A) The organs and blood samples were obtained from the PRV-Samal-24-1.0×10^5 PFU

mice on the 5th DPI (5 mice per group). The left and right panels indicate the viral RNA loads in the organs and the blood of the mice, respectively. Four PRV-Samal-24-1.0×10^5 PFU mice were sacrificed on the 5th DPI due to the humane endpoint. Another mouse was found dead on the 5th DPI, therefore blood sample was not obtained. Therefore, the viral RNA loads in each organ and those in the blood were determined in 5 mice (right panel) and 4 mice (left panel), respectively. (B) The organs were obtained from the PRV-Samal-24-1.0×10^6 PFU mice on the 4th DPI (2 mice per group). UDL, under detection limit.

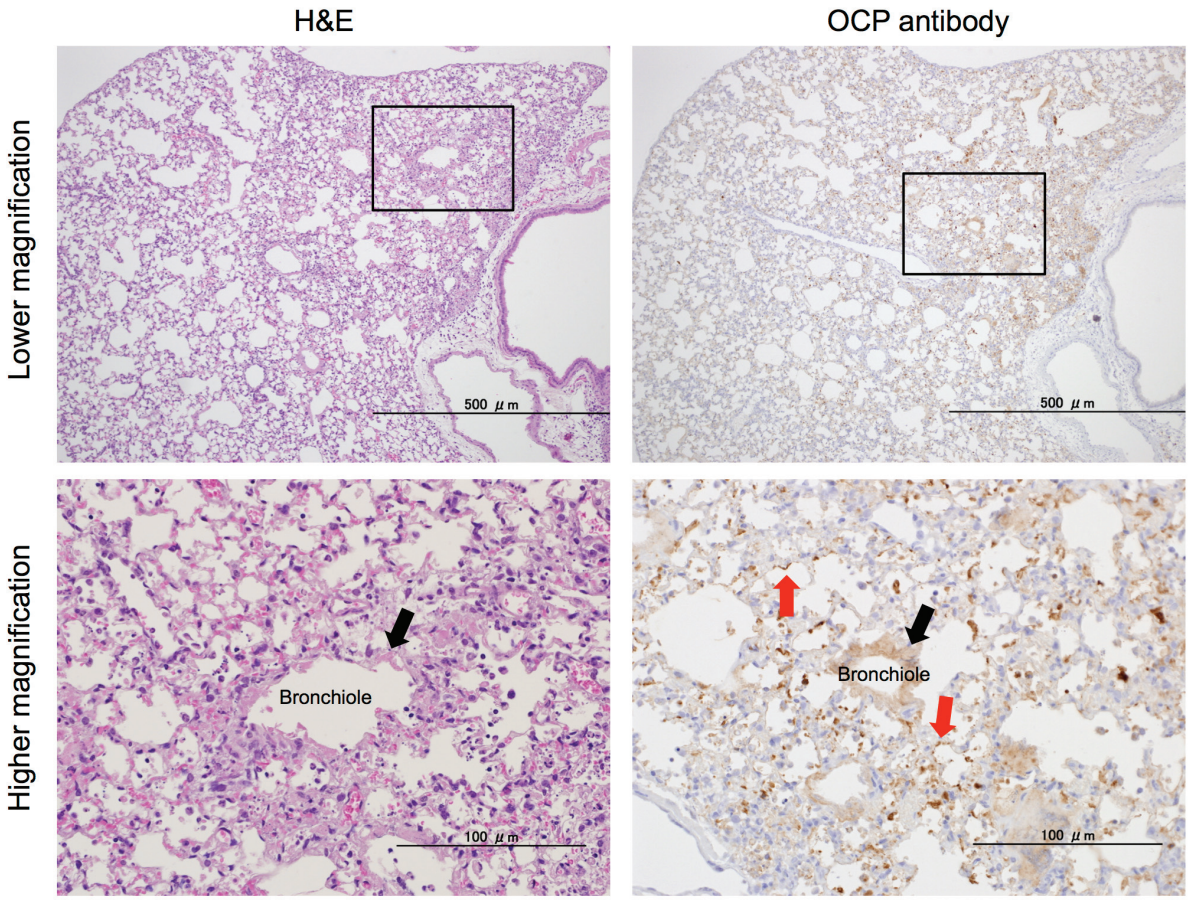

Figure 10. Histopathological findings of the lungs of BALB/c mice infected with PRV-Samal-24.

The lungs were obtained from PRV-Samal-24-1.0×10^6 PFU mice on the 4th DPI. H&E staining (left panels) and IHC with an OCP antibody (right panels) were performed. The H&E staining and IHC with an OCP antibody of the lung at 100× magnification (upper panels) and of a bronchiole and an alveolus at 400× magnification (lower panels) are shown. The black boxes in the upper panels were shown at higher magnification in the lower panels. The black arrows in the lower panels indicate the bronchiolar epithelial cell necrosis, which was positive for PRV-Samal-24 antigen. The red arrows in the lower-right panel indicate the PRV-Samal-24 antigen-positive pneumocytes. The scale bars in the upper panels indicate 500 μm, whereas those in the lower panels indicate 100 μm.

CHAPTER 2

Investigation of Immune Response to Pteropine Orthoreovirus (PRV) Infection and Evaluation of Therapeutic Efficacy of Anti-PRV Serum in PRV infection BALB/c Mouse Model

Summary

Lack of a proper animal model prevents development of preventive measures and therapeutics for Pteropine orthoreovirus (PRV) infection. Immune response in PRV infection BALB/c mouse model, which was developed respiratory disease due to PRV infection, was examined. Furthermore, efficacy of antiserum treatment for PRV infection was evaluated in PRV infection BALB/c mouse model. The serum neutralizing antibody titers induced in the BALB/c mice by the inoculation with non-lethal dose of human-borne PRV (PRV-MB) on the 27th day post-infection (DPI) were determined. The mice were then challenged with the lethal dose of PRV-MB on the 35th day after the first inoculation with a non-lethal dose of PRV-MB. Furthermore, BALB/c mice infected with lethal dose of PRV-MB were treated with PRV-MB-specific serum neutralizing antibodies. The serum neutralizing antibody titers induced in the mice inoculated with non-lethal dose of PRV-MB on the 27th DPI were between 640 and 2,560. All mice with immunity induced by pre-inoculation with a non-lethal dose of PRV-MB were completely protected from the lethal PRV-MB infection. Mice treated with antiserum with neutralizing antibody, which was produced in BALB/c mice by inoculation with PRV-MB 3 times, after inoculation with a lethal dose of PRV-MB showed a reduced fatality rate. These results suggest that vaccination is possible against PRV infection and neutralizing antibody can be used as a therapeutic agent. The PRV infection BALB/c mouse model can serve for evaluating the efficacy of prophylaxis and countermeasures, which will be developed to prevent and treat PRV infection.

Introduction

Pteropine orthoreovirus (PRV) was isolated from patients with respiratory tract infection (RTI). PRV is a bat-origin virus, whereas route of PRV infection and possibility of human-to-human transmission have not yet been elucidated. Antibodies to PRV were detected in 13.0% of residents of Tioman Island, Malaysia (11), and 4.4% of patients with nonspecific symptoms in central Vietnam (58). Furthermore, PRV genomes were detected in 17.0% of patients with RTIs in Negeri Sembilan state, Malaysia (66). There is a potential for PRV to cause RTIs in tropical or sub-tropical regions in Southeast Asia more widely than thought.

There are no vaccines and antiviral drugs for prevention and treatment against PRV infection. Animal models are essential for the development of preventive measures and therapeutics, whereas animal models of PRV infection, which are suitable for evaluating of the efficacy of vaccines and countermeasures, have not been developed. PRV infection BALB/c mouse model with RTI was developed (See in Chapter 1). In Chapter 2, immune response induced by infection with PRV was investigated in BALB/c mice. Therapeutic efficacy of antiserum with PRV-specific neutralizing antibody was also examined in BALB/c mice with lethal PRV infection.

Materials and Methods

Viruses

PRV, Miyazaki-Bali/2007 (PRV-MB), described in Chapter 1 (Materials and Methods), was used in this study.

Determination of infectious dose of PRV-MB with a plaque assay

The infectious dose of PRV-MB was determined in a plaque assay in Vero cell (ATCC, CCL-81) monolayers as described in Chapter 1 (materials and methods). The viral titers were calculated in plaque-forming units per milliliter (PFU/ml).

Mice

Nine-week-old female BALB/c mice (Japan SLC, Inc.) were used. The mice used were healthy and weighed approximately 20 g.

Determination of PRV-MB specific neutralizing antibody titer with a plaque reduction neutralization test

The PRV-MB specific serum neutralizing antibody titer was determined in a plaque reduction neutralization test (PRNT) in Vero cell monolayers as described previously (58,63). Serum samples were diluted 4-fold in Dulbecco's modified eagle's medium (DMEM; Sigma-Aldrich Co., LLC) supplemented with 2% heat-inactivated fetal bovine serum (FBS), 1% antibiotics (penicillin and streptomycin; Pen-Strep, Thermo Fisher Scientific, Inc.) (DMEM-2FBS) from 40 to 40,960. Each test sample was then mixed with the same volume of DMEM-2FBS containing PRV-MB at the infectious dose of 100 PFU and the mixture was

incubated for 1 h at 37 °C for neutralization. After incubation, the mixtures were tested with a plaque assay as described above, The neutralization titer was defined as the concentration of serum to reduce the number of plaques by 50% compared to that with control serum.

Protection of mice from lethal PRV-MB infection by induction of immunity to the virus

Five mice were intranasally inoculated with either DMEM-2FBS containing 1.0×10^3 PFU (non-lethal dose) of PRV-MB or DMEM-2FBS (control). Peripheral blood samples were collected through the caudal vein on the 27th DPI and sera were separated by centrifugation. The serum was tested for the PRV-MB neutralizing antibody titers with a PRNT as described above. In addition, mice that were pre-inoculated with PRV-MB or control were re-inoculated with 1.0×10^5 PFU (lethal dose) of PRV-MB on the 35th day after the first inoculation with PRV-MB or control. The clinical signs and body weight were monitored for 14 days. The mice that showed >25% initial body weight loss were euthanized. Their body weight changes and survival rates were plotted using the GraphPad Prism software program (GraphPad Software, Inc.).

Treatment of mice with antiserum after lethal PRV-MB infection

Twenty-five mice were intranasally inoculated with 1.0×10^3 PFU (non-lethal dose) of PRV-MB followed by a second intranasal inoculation with 1.0×10^5 PFU of PRV-MB 3 weeks after the first infection. The mice were then intranasally inoculated once more with 1.0×10^5 PFU of PRV-MB 3 weeks after the second infection. On the 5th day after the third inoculation, the mice were sacrificed and blood was collected by cardiac puncture. Serum was separated by centrifugation. Mouse sera, which were collected from the 25 control mice without inoculation with PRV-MB, were used as the control serum. The serum with a PRV-MB-specific neutralizing antibody titer of 10,240 was diluted 4-fold with PBS. Five

mice per group were intranasally infected with 1.0×10^5 PFU of PRV-MB, and then the diluent of the serum (100 μL) was intraperitoneally administered once daily until the mice showed >25% initial body weight loss for a maximum of 5 days. Serum was administered just after 1 h after inoculation with PRV-MB, or on the 1st, 2nd, 3rd, and 4th DPI. The diluent of the control serum (100 μL) was used for mock treatment. The mice that showed >25% initial body weight loss were euthanized. The body weight changes and survival rates were plotted using the GraphPad Prism software program.

Results

Protection from lethal PRV-MB infection by induction of immune response to PRV-MB in mice

The serum neutralizing antibody titers induced in the mice inoculated with 1.0×10^3 PFU (non-lethal dose) of PRV-MB on the 27th DPI were between 640 and 2560. The mice were then challenged with 1.0×10^5 PFU of PRV-MB on the 35th day after the first inoculation with a non-lethal dose of PRV-MB. All of these mice survived, whereas all of the control mice died by the 6th DPI (Figure 11).

Efficacy of antiserum in the treatment of PRV-MB infection in mice

A mixture of the serum sample collected from mice infected with PRV-MB was used as an antiserum with PRV-MB-specific neutralizing antibody titer of 10,240. The administration of antiserum to mice that had been infected with 1.0×10^5 PFU of PRV-MB showed a protective effect: the survival rate of the mice initiated antiserum treatment just after 1 h after inoculation with PRV-MB was 60% (Figure 12B) and that initiated antiserum treatment both on the 1st and 2nd DPI, taking the day on which the mice were infected with PRV-MB as day 0, was 40% (Figure 12C and D). Tthe control mice and the mice in which the antiserum treatment was initiated on the 3rd and 4th DPI, died by the 6th DPI (Figure 12A, E and F). The body weight reduction in these groups was similar to that of the control.

Discussion

Immunity to PRV-MB was induced by infection with non-lethal dose of PRV-MB and protected the mice from lethal infection with PRV-MB challenged (Figure 11), indicating that vaccination strategy might be possible against PRV infection.

The antiserum used in this study showed high PRV-MB specific neutralizing antibody titers (10,240). The antiserum treatment might result in suppressive effects against PRV-MB replication in BALB/c mice. The early initiation of the treatment could not protect BALB/c mice completely from lethal PRV-MB infection. The lungs of the mice, in which PRV-MB was mainly replicated (See in Chapter 1), might be infected with PRV-MB just 1 h after inoculation. On the 3rd DPI or later, infection with PRV-MB was extensive from bronchial epithelium to alveoli and caused severe respiratory disease in the mice (See in Figure 5B in Chapter 1). Therefore, the initiation of the treatment on the 3rd DPI or later failed to induce therapeutic efficacy in the mice infected with lethal dose of PRV-MB (Figure 12E and F). The early antiserum treatment with PRV-MB specific neutralizing antibody may be used as a therapeutic measure for PRV infection in humans.

All the cases of PRV infection in humans showed symptoms associated with RTI, whereas it is evident that the clinical characteristics of PRV infections in humans have not yet been elucidated. Therapeutic agents and vaccines should be developed to manage PRV-infections in humans. The PRV infection BALB/c mouse model may be useful not only for the evaluation of the potential pathogenicity of PRV, but also for that of the efficacy of vaccine and therapeutic candidates.

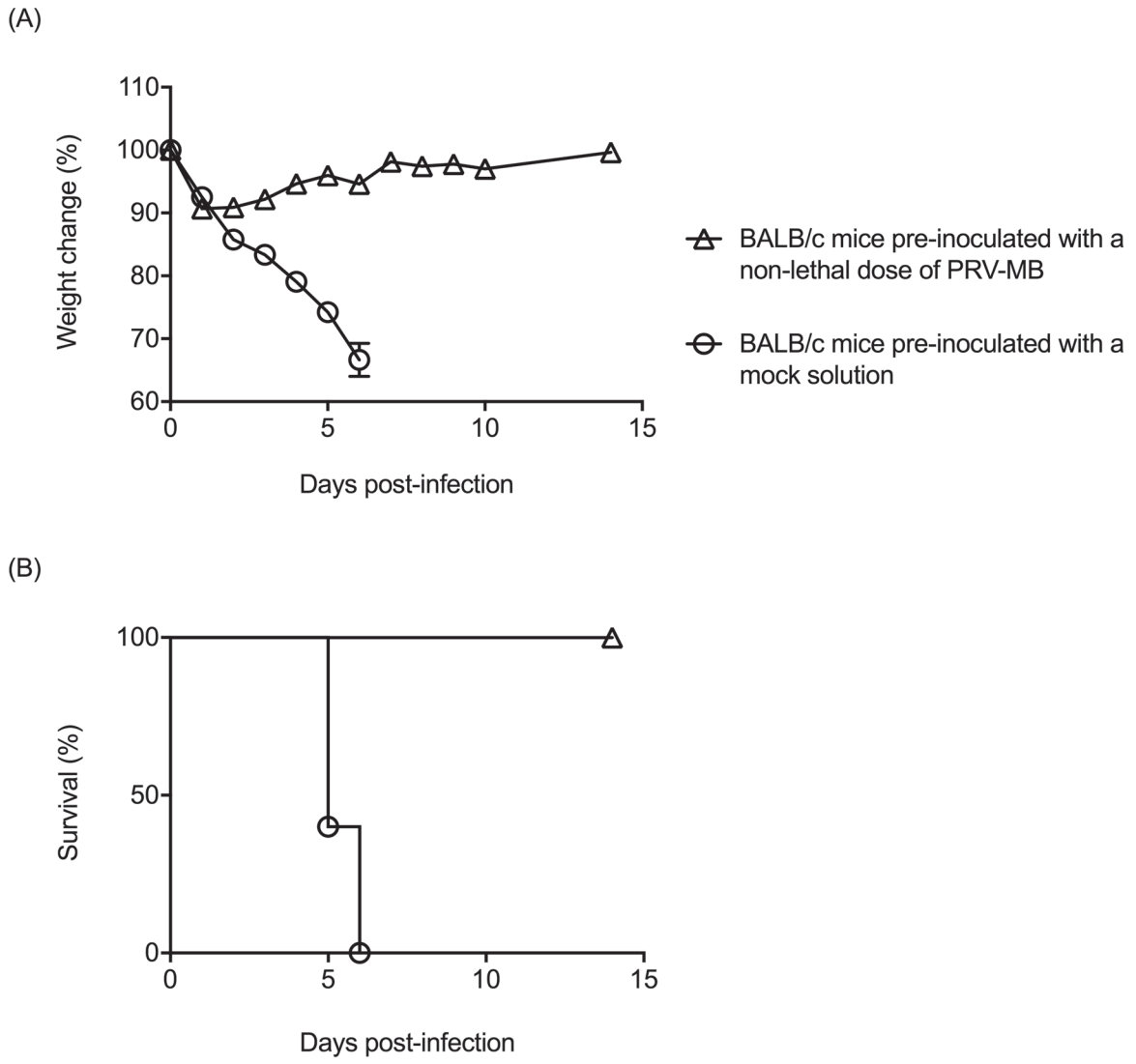

Figure 11. Changes in the body weight (A) and survival rate (B) in BALB/c mice challenged with a lethal dose of PRV-MB after non-lethal PRV-MB infection.

BALB/c mice were pre-inoculated with a non-lethal dose (1.0×10^3 PFU) of PRV-MB or with mock solution, followed by infection with 1.0×10^5 PFU of PRV-MB on the 35th day after the first inoculation (5 mice per group). Error bars indicate the standard error.

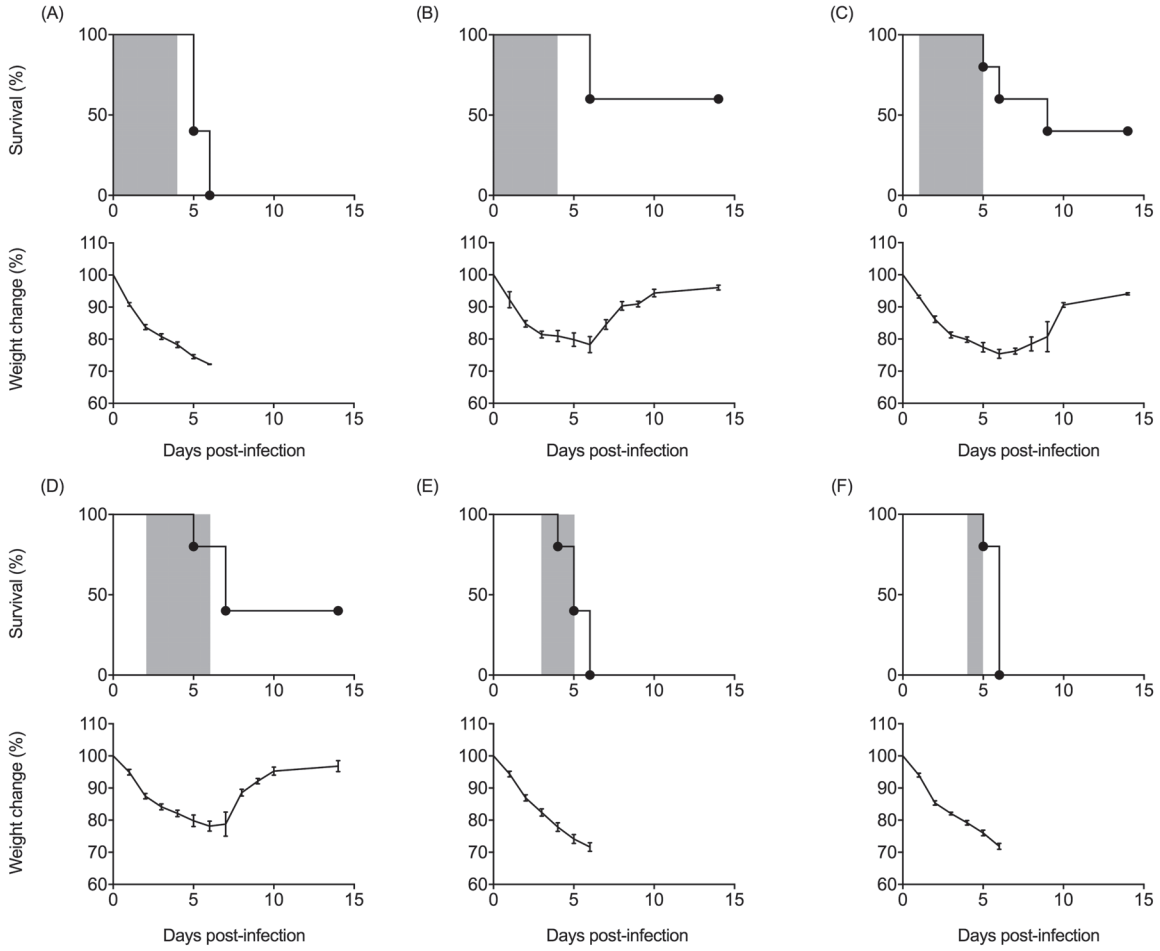

Figure 12. Changes in the survival rate (upper panels) and body weight (lower panels) in BALB/c mice treated with antiserum after lethal PRV-MB infection.

The PRV-MB-1.0×10^5 PFU mice were treated with the intraperitoneal administration of antiserum once daily during periods surrounded by the gray boxes (5 mice per group). Antiserum with a PRV-MB-specific serum neutralizing antibody titer of 10,240 was diluted 4-fold with saline. The volume of the antiserum administered daily was 100 μL. The treatment was initiated just after 1 h after the virus challenge (B) or from the 1st (C), 2nd (D), 3rd (E), and 4th (F) DPI. The control mice were administrated with the same volume of control serum diluted with PBS (A). Error bars indicate the standard error.

CHAPTER 3

Inhibitory efficacy of Ribavirin for Pteropine Orthoreovirus (PRV) Replication *in Vitro* and its Evaluation as a Therapeutic Agent for PRV Infection *in Vivo*

Summary

It was demonstrated that Pteropine orthoreovirus (PRV) is a causative agent of respiratory tract infection. However, the clinical characteristics of PRV infections in humans have not yet been elucidated. Therapeutic agents for PRV infection should be developed. Therapeutic candidate drugs against PRV infection were screened with a chemical library in human hepatoma cells (Huh-7 cells). Ribavirin showed an inhibitory effect on the PRV replication and was considered as a therapeutic candidate. Ninety % inhibitory concentrations (IC_{90}) of the ribavirin for PRV (PRV-MB) replication were determined to be 100 μM and 369 μM in Huh-7 cells and Vero cells, respectively. Those against bat-borne PRV (PRV-Samal-24) replication were also determined to be 81 μM and 346 μM in Huh-7 cells and Vero cells, respectively. However, all BALB/c mice treated with ribavirin (100 mg/kg/day) after infection with lethal dose of PRV-Samal-24 died by 5th day post-infection. Ribavirin was determined to have an inhibitory effect on PRV replication *in vitro*, whereas it did not show any efficacy in the treatment of BALB/c mice with lethal PRV infection. Although ribavirin showed an inhibitory effect on PRV replication *in vitro*, it did not show any therapeutic efficacy *in vivo*. These results suggest that a drug with *in vitro* inhibitory effect does not always show a therapeutic efficacy.

Introduction

It was demonstrated that Pteropine orthoreovirus (PRV) is a causative agent of respiratory tract infection (RTI) on the basis of Koch's postulations (See in Chapter 1). However, the clinical characteristics of PRV infections in humans have not yet been elucidated. Antiserum treatment with PRV-specific neutralizing antibody was effective for PRV infection, whereas it did not protect BALB/c mice completely from lethal PRV infection (See in Chapter 2). Development of other therapeutic agents than the antiserum, is required.

Virions of mammalian orthoreovirus (MRV) classified into *Orthoreoviridae* similarly to PRV, are composed of two concentric protein shells, the outer capsid and core proteins. MRV entry into the host cells is initiated through an attachment of the cell attachment protein (CAP) with the cell-surface receptors (6,37,67). The CAP attaches with at least two different receptors, sialic acid-containing glycans (2,6,18,45,47) and junctional adhesion molecule-A (4,6,8,51). Through the CAP-receptor binding, virions are internalized via a β1 integrin-dependent process into endosomes (6,39), where virion disassembly occurs (23,39). During disassembly, the CAP and outer-capsid protein (OCP) are removed, exposing major outer-capsid protein (MOCP), which is subsequently cleaved. Proteolysis of the MOCP results in conformational rearrangements that facilitate endosomal membrane rupture and delivery of transcriptionally active core particles into the cytoplasm (6,43,44). Primary transcription occurs within the viral core, and nascent RNAs are translated or encapsidated into new viral cores, at which nascent RNAs serve as templates for negative-strand viral RNA synthesis. Within new viral cores, secondary rounds of transcription occur. The OCP coalesce onto nascent particles to generate progeny virions, which are released by an unknown mechanism.

The CAP of PRV affects replication *in vitro* (32) similarly to MRV. However, the replication mechanism of PRV remains unknown in detail. Therefore, it is difficult to specify the viral proteins, with which candidate drugs should be interacted. Cell-based screening methods with the use of chemical libraries were then developed for identification of potential therapeutic agents against influenza A virus (IAV) and coronavirus (CoV) with some modifications (9,17). It is worth of note that promising drugs against virus infections, for which therapeutics have not been reported, can be selected by screening of chemical libraries.

In Chapter 3, a screening for therapeutic candidates against PRV infection was performed with the use of a chemical library, which included biologically annotated collection of inhibiters, receptor ligands, pharma-developed tools, and approved drugs. Therapeutic candidates for IAV and those for CoV were detected in chemical libraries with use of a recombinant green fluorescent protein-expressing IAV and a recombinant luciferase-expressing CoV, respectively (9,17), whereas those for PRV infection were detected with use of a cell proliferation reagent. A broad-spectrum antiviral drug ribavirin (1-β-D-ribofuranosyl-1, 2, 4-triazole-3-carboxamide and a guanosine analogue), which has a therapeutic efficacy for Lassa fever and hepatitis C (24,40), was detected as a candidate against PRV infection. The therapeutic efficacy of ribavirin was evaluated in the PRV infection BALB/c mouse model developed (See in Chapters 1and 2).

Materials and Methods

Viruses

Two PRV strains, PRV, Miyazaki-Bali/2007 (PRV-MB), and bat-borne PRV, Samal-24 (PRV-Samal-24) described in Chapter 1, were used.

Determination of infectious dose of PRV-MB and PRV-Samal-24 with a plaque assay

The infectious dose of each virus was measured with a plaque assay in Vero cell (ATCC, CCL-81) monolayers as described in Chapter 1. The viral titers were calculated in plaque-forming units per milliliter (PFU/ml).

Chemical compounds

The library of pharmacologically active compounds (SIGMA LOPAC^{1280}, Sigma-Aldrich Co., LLC) including biologically annotated collection of inhibiters, receptor ligands, pharma-developed tools, and approved drugs, was used. A total of 1280 chemical compounds was included in the library. Each compound at the concentration of 10 mM in 100% dimethyl sulfoxide (DMSO) was stored at -80°C until use.

Selection of chemical compounds with inhibitory effect on PRV-MB replication

The 10 mM compounds were diluted 50-fold in Dulbecco's modified eagle's medium (DMEM; Sigma-Aldrich Co., LLC) supplemented with 2% heat-inactivated fetal bovine serum (FBS) and 1% antibiotics (penicillin and streptomycin; Pen-Strep, Thermo Fisher Scientific, Inc.) (DMEM-2FBS). The inhibitory effect of each chemical compound on PRV-MB replication was examined with a 96-well plate format using human hepatoma cells (Huh-7 cells). Approximately 4.0×10^2 Huh-7 cells per well were seeded and cultivated at

37°C for 24 h. The growth medium (DMEM supplemented with 5% FBS and 1% antibiotics, DMEM-5FBS) was replaced with 50 µl of DMEM-2FBS containing each 200 µM compound, and then 50 µl of DMEM-2FBS containing 5 PFU of PRV-MB were added to each well. The final concentration of each compound in each well was 100 µM. One hundred µl of DMEM-2FBS containing 5 PFU of PRV-MB and 1% DMSO was added to the control wells. The cells were cultivated at 37°C for 2 days, and then cell viability was determined using the WST-1 (Roche Diagnostics, Ltd.) according to the manufacture's protocol. The WST-1 was diluted 2-fold in phosphate buffered saline (PBS). The diluted WST-1 was added to the cells, followed by incubation at 37°C for 45 min. Absorbance was measured and chemical compounds that showed the absorbance of >1.500, at which no cytopathic effect appeared in Huh-7 cells, were selected as candidate inhibitors for PRV-MB replication. To confirm the inhibitory effect of the chemical compounds detected in the 1st screening on the PRV-MB replication, the inhibitory effect of the candidate selected were evaluated with the same method described above. The cytotoxicity of the candidate drugs selected was examined as described below.

Evaluation of cytotoxicity of the chemical compounds

Cytotoxicity of two compounds, ribavirin (YAMASA Co., Ltd.) and gemcitabine hydrochloride (Tokyo Chemical Industry Co., Ltd.), were determined using the WST-1 (55). The cells were cultivated for 3 days in the presence or absence of the compound without virus inoculation, and cell viability was measured using the WST-1. Cell viability was calculated as follows: (absorbance of cells in the presence of the compound – absorbance of no cells in the presence of the compound) / (absorbance of cells in the absence of the compound – absorbance of no cells in the absence of the compound) × 100 (%). The cell viability was plotted using the GraphPad Prism software program (GraphPad Software, Inc.).

Determination of 90% inhibitory concentration of anti-PRV drug candidates, ribavirin and gemcitabine hydrochloride, for PRV in Huh-7 cells and Vero cells

The 90% inhibitory concentrations (IC_{90}) of ribavirin for PRV-MB and PRV-Samal-24 replication were determined both in Huh-7 cells and in Vero cells. The IC_{90} of gemcitabine hydrochloride for PRV-MB replication was also determined both in Huh-7 cells and in Vero cells. The cells were inoculated with PRV-MB at the multiplicity of infection (m.o.i) of 1.0×10^{-2} of the virus, followed by incubation at 37℃ for 1 h. After removal of the virus-containing medium, the cells were cultured for 3 days in DMEM-2FBS with each of the drug, ribavirin and gemcitabine hydrochloride, at the designated concentrations. The designated concentrations were 0.1, 1.0, 10.0, 100.0, and 1000.0 μM. The medium was centrifuged at 800 × *g* for 5 min to remove cellular debris. The supernatant was collected and stored at -80°C until use. The viral titers were determined with a plaque assay as described above (69). The IC_{90} of ribavirin and gemcitabine hydrochloride for PRV replication were calculated using the reduction curves plotted. The effect of PRV replication was calculated by plotting the infectious dose of PRV using the GraphPad Prism software program.

Treatment of BALB/c mice with ribavirin after lethal PRV infection

Nine-week-old BALB/c mice (Japan SLC, Inc.), which were anesthetized with a combination of ketamine (100 mg/kg) and xylazine (4 mg/kg) in 0.9% sodium chloride solution, were inoculated with 1.0×10^5 PFU (lethal dose) of PRV-Samal-24 intranasally. Then the mice were administered with 100 μl of ribavirin (100 mg/kg/day) diluted with PBS intraperitoneally once daily for 3 days. Administration of ribavirin was initiated just after 1 h from the virus inoculation, or on the 1st, 2nd, 3rd day post-infection (DPI). One hundred μl of PBS was used for mock treatment. The mice, which showed >25% initial body weight loss,

were euthanized. The body weight changes and survival rates were plotted using the GraphPad Prism software program.

Results

Inhibition of ribavirin and gemcitabine hydrochloride on PRV-MB replication in Huh-7 cells

The set of SIGMA LOPAC[1280] was examined for the inhibitory effect on PRV-MB replication in Huh-7 cells. In the 1st screening, the PRV-MB-infecting Huh-7 cells (PRV-MB-Huh-7) showed a higher absorbance of >1.500 when cultured in the presence of Mifepristone, Artrnether, Retinoic acid, BMY7378 dihydrochloride, ribavirin, N,N-Dihexyl-2-(4-uorophenyl) indole 3-acetamide, NBI27914, gemcitabine hydrochloride, AGK2, and MRS 1523, being the absorbance values 1.520, 1.524, 1.534, 1.590, 1.654, 1.691, 1.691, 1.696, 2.065, and 2.166, respectively. The absorbance values of PRV-MB-Huh-7 cultured in the presence of the other drugs were less than 1.500, a cut-off value. The 10 candidates were tested for antiviral effect with the same screening method again. Absorbance of PRV-MB-Huh-7 in the presence of gemcitabine hydrochloride and ribavirin were determined to be 1.690 and 2.238, respectively, whereas these cultured in the presence of the other drugs were determined to be less than 1.500. Finally, ribavirin and gemcitabine hydrochloride were selected for further evaluation.

Determination of IC_{90}S of ribavirin and gemcitabine hydrochloride for PRV replication in Huh-7 cells and Vero cells

Ribavirin inhibited PRV-MB replication both in Huh-7 cells and in Vero cells in a dose dependent manner (Figure 13A and B). The IC_{90} of ribavirin to PRV-MB was determined to be 100 μM and 369 μM in Huh-7 cells and Vero cells, respectively. It also inhibited

PRV-Samal-24 replication, being the IC_{90} of the ribavirin to PRV-Samal-24 81 μM and 346 μM in Huh-7 cells and Vero cells, respectively. The cell viability of Huh-7 cells and Vero cells cultured in the presence of ribavirin at the concentration, which ribavirin showed inhibitory effect on PRV replication, was maintained (Figure 13A and B).

Gemcitabine hydrochloride also inhibited PRV-MB replication in a dose dependent manner (Figure 13C and D). The IC_{90} of gemcitabine hydrochloride to PRV-MB was determined to be 0.8 μM in Huh-7 cells, while the 50% cytotoxicity of the drug to Huh-7 cells was over 1000.0 μM. To the contrary, the IC_{90} of the drug to PRV-MB was determined to be 0.3 μM in Vero cells, while the 50% cytotoxicity of the drug to Vero cells was less than 0.1 μM (Figure 13C and D).

Therapeutic efficacy of ribavirin for PRV infection in BALB/c mice

Administration of BALB/c mice (5 mice per group) with ribavirin (100 mg/kg/day), for 4 days, intraperitoneally just after infection with lethal dose (1.0×10^5 PFU) of PRV-Samal-24 showed no any protective effects (Figure 14). All the mice died by the 5th DPI. The body weight reduction in ribavirin-treated group was also similar to that in the mock-treated group.

Discussion

Ribavirin and gemcitabine hydrochloride among the chemical library inhibited PRV replication *in vitro*.

The IC_{90} of ribavirin to Vero cells were higher than that to Huh-7 cells, suggesting that Vero cells were less sensitive to ribavirin than other several cell lines as reported previously (53,55). Ribavirin was reported to inhibit mammalian orthoreovirus (MRV), which is classified into the same genus as PRV. The IC_{90} for MRV replication was reported to be 12.5 μM in mouse L929 fibroblasts cells (53). The mechanism of action of ribavirin has not well known. There are 4 possible antiviral mechanism of action of ribavirin: 1. reduction of intracellular guanosine triphosphate (GTP) by inhibition of inosine monophosphate dehydrogenase; 2. increase in mutagenesis to viral genomes by decrease in GTP pool; 3. interference of increased ribavirin triphosphate (RTP) with viral RNA polymerase; 4. viral mRNA capping inhibition (46,55). It has also been suggested that the action of ribavirin on MRV proliferation was mainly due to the inhibitory action of RTP on viral RNA polymerase and the helicase activity of the transcriptase (53). Given the fact that both PRV and MRV belong to the same genus, mechanisms of action of ribavirin on PRV might be similar to those of MRV. Ribavirin inhibited PRV replication *in vitro*, but did not show any therapeutic efficacy in the PRV infection BALB/c mouse model, which was developed in this study (Figure 14).

The dose of ribavirin in the present study was 100 mg/kg/day because the ribavirin dose was used in the other studies, in which ribavirin efficacy for the treatment of some other virus infection was evaluated (62).

Gemcitabine hydrochloride (2',2'-difluoro-2'-deoxycytidine) is a deoxycytidine analogue, which is a therapeutic agent for non-small cell lung cancer and pancreatic cancer (16,29,49).

Gemcitabine hydrochloride was reported to show inhibitory effect on several RNA and DNA viruses, such as human immunodeficiency virus type 1, murine leukemia virus, IAV, and herpes simplex virus type 1 (14,15,17). Gemcitabine hydrochloride inhibited PRV-MB replication in Huh-7 cells at the concentration of 10.0 μM, at which the cell viability was maintained 97% on average. However, the cytotoxicity of gemcitabine hydrochloride was strong against Vero cells. It seems that the antiviral effect on PRV in Vero cells might be associated with the strong cytotoxicity to Vero cells (Figure 13). Therefore, gemcitabine hydrochloride was not considered to be a therapeutic candidate.

In conclusion, ribavirin and gemcitabine hydrochloride showed inhibitory effect on the PRV replication *in vitro*, however ribavirin did not show any therapeutic effect in the treatment of PRV infection *in vivo*. It was demonstrated that a drug with *in vitro* inhibitory effect does not always show a therapeutic efficacy *in vivo*.

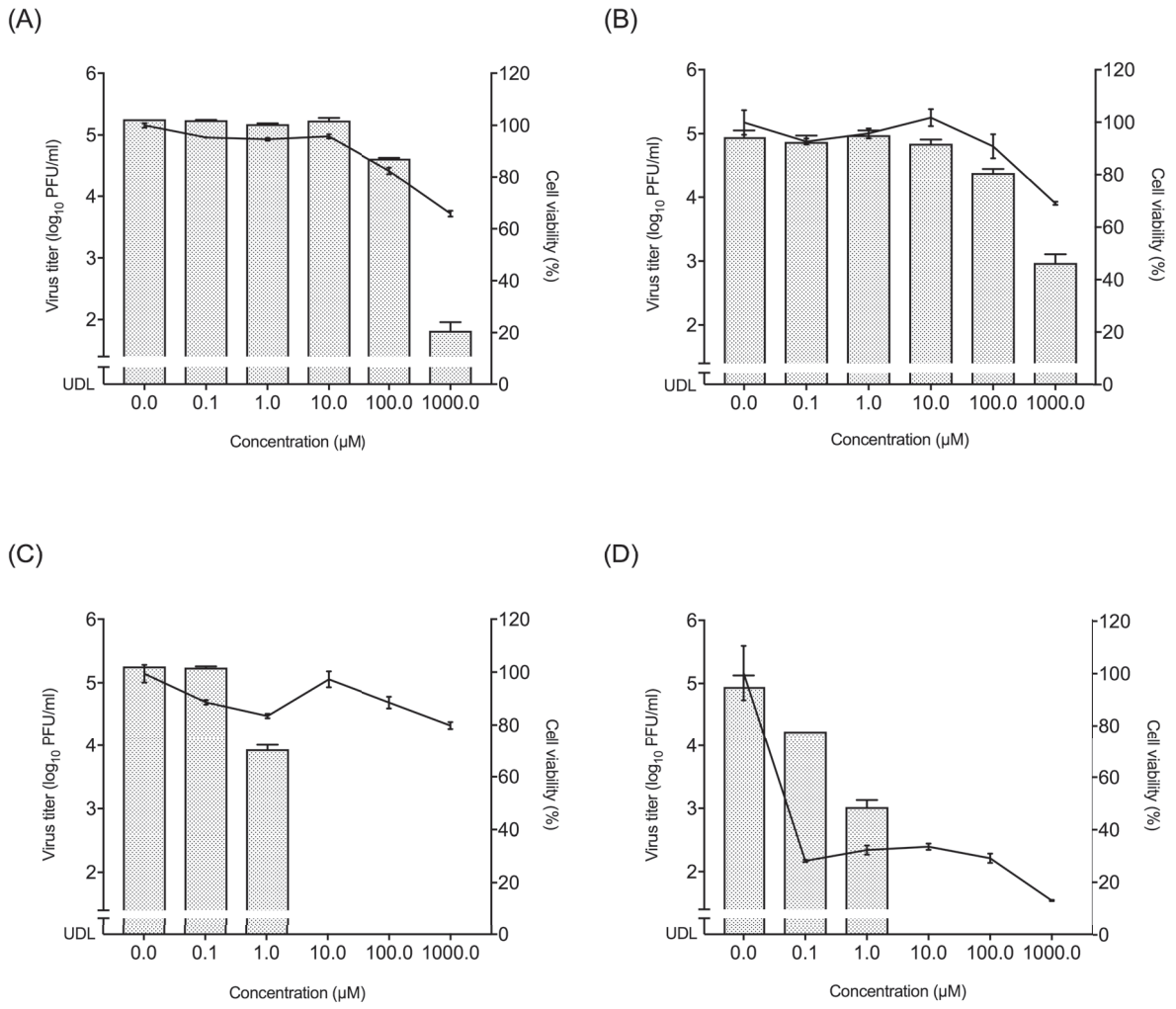

Figure 13. Effects of ribavirin and gemcitabine hydrochloride on PRV-MB replication and on cell viability.

The bars indicate the infectious dose level of PRV-MB at the designated concentrations of the drugs tested (left y-axis). The polygonal lines indicate the cell viability at the designated concentrations of the drugs tested (right y-axis). PRV-MB replication and cell viability in Huh7 cells in the presence of the ribavirin (A), those in Vero cells in the presence of the ribavirin (B), those in Huh7 cells in the presence of the gemcitabine hydrochloride (C), and those in Vero cells in the presence of the gemcitabine hydrochloride (D) were shown. Experiments were performed in triplicate and error bars indicate the standard error. UDL, under detection limit.

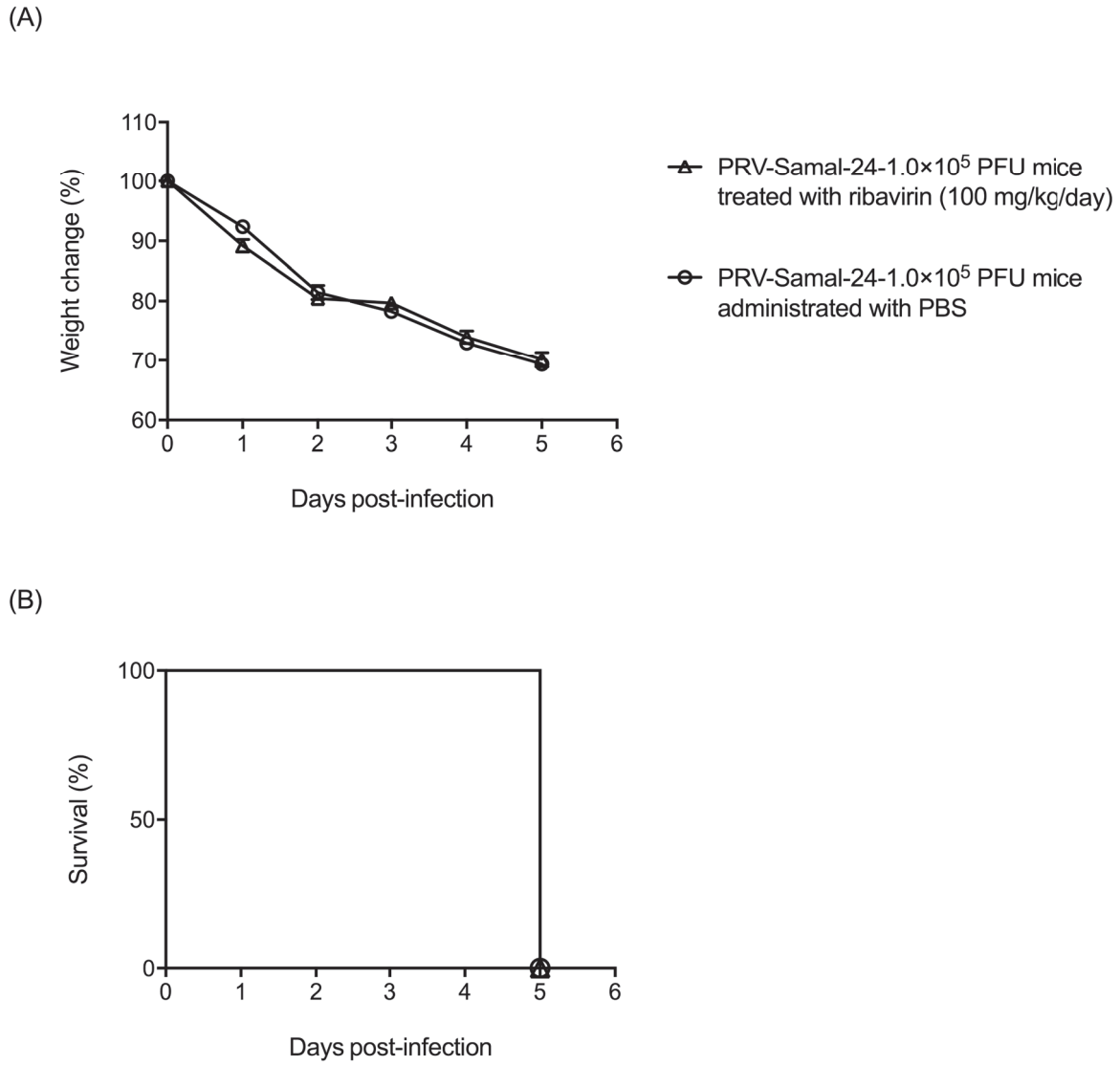

Figure 14. The changes in the body weight (A) and survival rate (B) of BALB/c mice treated with ribavirin after lethal PRV-Samal-24 infection.

The mice infected with 1.0×10^5 PFU of PRV-Samal-24 (PRV-Samal-24-1.0×10^5 PFU mice) were administered with ribavirin (100 mg/kg/day) through the intraperitoneal route just after 1 h after the virus challenge once daily for 3 days. The negative control mice (PRV-Samal-24-1.0×10^5 PFU mice) were administered with PBS. Error bars in Figure 14 (A) indicate the standard error.

CONCLUSIONS

The objective of this study was to develop Pteropine orthoreovirtus (PRV) infection BALB/c mouse model for analyzing the pathogenicity of PRV and for evaluating the efficacy of vaccines and therapeutic agents against PRV infection. The results obtained were written described as follows.

1. The intranasal inoculation of BALB/c mice with PRV (PRV-MB), which was isolated from a Japanese patient with respiratory tract infection, caused lethal respiratory disease. The 50% lethal dose (LD_{50}) of PRV-MB was 6.8×10^3 PFU/head. Viral RNA was amplified with high degree in the lungs, and pathological changes were demonstrated in the bronchiole and alveoli.

2. The intranasal inoculation of BALB/c mice with bat-borne PRV (PRV-Samal-24) also caused respiratory disease similarly to those with PRV-MB. The LD_{50} of PRV-Samal-24 was 4.2×10^3 PFU/head.

3. All mice with immunity induced by pre-inoculation with a non-lethal dose of PRV were completely protected against lethal PRV infection.

4. The mice infected with a lethal dose of PRV showed a reduced fatality rate by the treatment with antiserum with neutralizing antibody activity.

5. Ribavirin and gemcitabine hydrochloride were selected as therapeutic agent against PRV infection from a chemical library. Ribavirin and gemcitabine hydrochloride showed

inhibitory effect on the PRV replication *in vitro*, however ribavirin did not show any therapeutic effect in the treatment of PRV infection *in vivo*.

The PRV infection BALB/c mouse model with respiratory disease was first developed. This model facilitates the *in vivo* study on PRV infection and basic virology on PRV.

ACKNOWLEDGEMENTS

I wish to express my gratitude to Masayuki Saijo, MD, PhD, Director, Department of Virology 1, NIID, for his valuable discussion for completion of this manuscript. I also wish to thank Dr. Shuetsu Fukushi, Department of Virology 1, NIID, for his valuable discussion and technical advice. I am indebted to Dr. Masayuki Shimojima, Dr. Satoshi Taniguchi, Dr. Hideki Tani, Dr. Tomoki Yoshikawa, Dr. Takeshi Kurosu, and Dr. Shumpei Watanabe (Department of Virology 1, NIID), and Dr. Noriyo Nagata (Department of Pathology, NIID), for their helpful discussion and technical advice.

I appreciate Professor Tetsuya Mizutani, DVM, PhD, Research and Education Center for Prevention of Global Infectious Disease of Animal, Tokyo University of Agriculture and Technology, for his valuable comments. I thank Dr. Singh Harpal and Dr. Aiko Fukuma (Department of Virology 1, NIID), and Ms. Ayako Harashima and Ms. Yuko Sato (Department of Pathology, NIID) for their technical assistance. I am also grateful to Dr. Ken Maeda (Laboratory of Veterinary Microbiology, Joint Faculty of Veterinary Medicine, Yamaguchi University), Dr. Shigeru Kyuwa (Department of Biomedical Science, Graduate School of Agricultural and Life Sciences, The University of Tokyo), Dr. Taisuke Horimoto (Department of Veterinary Microbiology, Graduate School of Agricultural and Life Sciences, The University of Tokyo), and Dr. Yasuhiro Yoshikawa (Department of Animal Risk Management, Chiba Institute of Science) for permission to use PRV-Samal-24. I also thank Ms. Momoko Ogata, and Ms. Junko Hirai for their great clerical assistance. Finally, I am grateful to the members of the Department of Virology 1, NIID.

REFERENCES

1. Arashkia A, Roohvand F, Memarnejadian A, Aghasadeghi MR, Rafati S. (2010). Construction of HCV-polytope vaccine candidates harbouring immune-enhancer sequences and primary evaluation of their immunogenicity in BALB/c mice. Virus Genes 40, 44~52.
2. Armstrong GD, Paul RW, Lee PW. (1984). Studies on reovirus receptors of L cells: virus binding characteristics and comparison with reovirus receptors of erythrocytes. Virology 138, 37~48.
3. Arnold MM, Murray KE, Nibert ML. (2008). Formation of the factory matrix is an important, though not a sufficient function of nonstructural protein mu NS during reovirus infection. Virology 375, 412~423.
4. Barton ES, Forrest JC, Connolly JL, Chappell JD, Liu Y, Schnell FJ, Nusrat A, Parkos CA, Dermody TS. (2001). Junction adhesion molecule is a receptor for reovirus. Cell 104, 441~451.
5. Becker MM, Peters TR, Dermody TS. (2003). Reovirus sigma NS and mu NS proteins form cytoplasmic inclusion structures in the absence of viral infection. Journal of Virology 77, 5948~5963.
6. Boehme KW, Ikizler M, Kobayashi T, Dermody TS. (2011). Reverse genetics for mammalian reovirus. Methods (San Diego, Calif) 55, 109~113.
7. Broering TJ, Parker JS, Joyce PL, Kim J, Nibert ML. (2002). Mammalian reovirus nonstructural protein microNS forms large inclusions and colocalizes with reovirus microtubule-associated protein micro2 in transfected cells. Journal of Virology 76, 8285~8297.
8. Campbell JA, Schelling P, Wetzel JD, Johnson EM, Forrest JC, Wilson GA,

Aurrand-Lions M, Imhof BA, Stehle T, Dermody TS. (2005). Junctional adhesion molecule a serves as a receptor for prototype and field-isolate strains of mammalian reovirus. Journal of Virology 79, 7967~7978.

9. Cao J, Forrest JC, Zhang X. (2015). A screen of the NIH clinical collection small molecule library identifies potential anti-coronavirus drugs. Antiviral Research 114, 1~10.
10. Cheng P, Lau CS, Lai A, Ho E, Leung P, Chan F, Wong A, Lim W. (2009). A novel reovirus isolated from a patient with acute respiratory disease. Journal of Clinical Virology : the Official Publication of the Pan American Society for Clinical Virology 45, 79~80.
11. Chua KB, Crameri G, Hyatt A, Yu M, Tompang MR, Rosli J, McEachern J, Crameri S, Kumarasamy V, Eaton BT, Wang LF. (2007). A previously unknown reovirus of bat origin is associated with an acute respiratory disease in humans. Proceedings of the National Academy of Sciences of the United States of America 104, 11424~11429.
12. Chua KB, Voon K, Crameri G, Tan HS, Rosli J, McEachern JA, Suluraju S, Yu M, Wang LF. (2008). Identification and characterization of a new orthoreovirus from patients with acute respiratory infections. PloS One 3, e3803.
13. Chua KB, Voon K, Yu M, Keniscope C, Abdul Rasid K, Wang LF. (2011). Investigation of a potential zoonotic transmission of orthoreovirus associated with acute influenza-like illness in an adult patient. PloS One 6, e25434.
14. Clouser CL, Holtz CM, Mullett M, Crankshaw DL, Briggs JE, Chauhan J, VanHoutan IM, Patterson SE, Mansky LM. (2011). Analysis of the ex vivo and in vivo antiretroviral activity of gemcitabine. PloS One 6, e15840.
15. Clouser CL, Holtz CM, Mullett M, Crankshaw DL, Briggs JE, O'Sullivan MG, Patterson SE, Mansky LM. (2012). Activity of a novel combined antiretroviral therapy of

gemcitabine and decitabine in a mouse model for HIV-1. Antimicrobial Agents and Chemotherapy 56, 1942~1948.

16. Comella P, Frasci G, Panza N, Manzione L, De Cataldis G, Cioffi R, Maiorino L, Micillo E, Lorusso V, Di Rienzo G, Filippelli G, Lamberti A, Natale M, Bilancia D, Nicolella G, Di Nota A, Comella G. (2000). Randomized trial comparing cisplatin, gemcitabine, and vinorelbine with either cisplatin and gemcitabine or cisplatin and vinorelbine in advanced non-small-cell lung cancer: interim analysis of a phase III trial of the Southern Italy Cooperative Oncology Group. Journal of Clinical Oncology : Official Journal of the American Society of Clinical Oncology 18, 1451~1457.
17. Denisova OV, Kakkola L, Feng L, Stenman J, Nagaraj A, Lampe J, Yadav B, Aittokallio T, Kaukinen P, Ahola T, Kuivanen S, Vapalahti O, Kantele A, Tynell J, Julkunen I, Kallio-Kokko H, Paavilainen H, Hukkanen V, Elliott RM, De Brabander JK, Saelens X, Kainov DE. (2012). Obatoclax, saliphenylhalamide, and gemcitabine inhibit influenza a virus infection. The Journal of Biological Chemistry 287, 35324~35332.
18. Dermody TS, Nibert ML, Bassel-Duby R, Fields BN. (1990). A sigma 1 region important for hemagglutination by serotype 3 reovirus strains. Journal of Virology 64, 5173~5176.
19. Dryden KA, Wang G, Yeager M, Nibert ML, Coombs KM, Furlong DB, Fields BN, Baker TS. (1993). Early steps in reovirus infection are associated with dramatic changes in supramolecular structure and protein conformation: analysis of virions and subviral particles by cryoelectron microscopy and image reconstruction. The Journal of Cell Biology 122, 1023~1041.
20. Du L, Lu Z, Fan Y, Meng K, Jiang Y, Zhu Y, Wang S, Gu W, Zou X, Tu C. (2010). Xi River virus, a new bat reovirus isolated in Southern China. Archives of Virology 155, 1295~1299.
21. Duncan R. (1999). Extensive sequence divergence and phylogenetic relationships

between the fusogenic and nonfusogenic orthoreoviruses: a species proposal. Virology 260, 316~328.

22. Duncan R, Corcoran J, Shou J, Stoltz D. (2004). Reptilian reovirus: a new fusogenic orthoreovirus species. Virology 319, 131~140.
23. Ebert DH, Deussing J, Peters C, Dermody TS. (2002). Cathepsin L and cathepsin B mediate reovirus disassembly in murine fibroblast cells. The Journal of Biological Chemistry 277, 24609~24617.
24. Feld JJ, Hoofnagle JH. (2005). Mechanism of action of interferon and ribavirin in treatment of hepatitis C. Nature 436, 967~972.
25. Gard G, Compans RW. (1970). Structure and cytopathic effects of Nelson Bay virus. Journal of Virology 6, 100~106.
26. Gard GP, Marshall ID. (1973). Nelson Bay virus. A novel reovirus. Archiv fur die Gesamte Virusforschung 43, 34~42.
27. Gauvin L, Bennett S, Liu H, Hakimi M, Schlossmacher M, Majithia J, Brown EG. (2013). Respiratory infection of mice with mammalian reoviruses causes systemic infection with age and strain dependent pneumonia and encephalitis. Virology Journal 10, 67.
28. Herzog EL, Brody AR, Colby TV, Mason R, Williams MC. (2008). Knowns and unknowns of the alveolus. Proceedings of the American Thoracic Society 5, 778~782.
29. Hidalgo M, Castellano D, Paz-Ares L, Gravalos C, Diaz-Puente M, Hitt R, Alonso S, Cortes-Funes H. (1999). Phase I-II study of gemcitabine and fluorouracil as a continuous infusion in patients with pancreatic cancer. Journal of Clinical Oncology : Official Journal of the American Society of Clinical Oncology 17, 585~592.
30. Hu T, Qiu W, He B, Zhang Y, Yu J, Liang X, Zhang W, Chen G, Zhang Y, Wang Y, Zheng Y, Feng Z, Hu Y, Zhou W, Tu C, Fan Q, Zhang F. (2014). Characterization of a novel orthoreovirus isolated from fruit bat, China. BMC Microbiology 14, 293.

31. Kaufmann SH, Schaible UE. (2005). 100th anniversary of Robert Koch's Nobel Prize for the discovery of the tubercle bacillus. Trends in Microbiology 13, 469~475.

32. Kawagishi T, Kanai Y, Tani H, Shimojima M, Saijo M, Matsuura Y, Kobayashi T. (2016). Reverse genetics for fusogenic bat-borne orthoreovirus associated with acute respiratory tract infections in humans: role of outer capsid protein sigmaC in viral replication and pathogenesis. PLoS Pathogens 12, e1005455.

33. Kim E, Okada K, Kenniston T, Raj VS, AlHajri MM, Farag EA, AlHajri F, Osterhaus AD, Haagmans BL, Gambotto A. (2014). Immunogenicity of an adenoviral-based middle east respiratory syndrome coronavirus vaccine in BALB/c mice. Vaccine 32, 5975~5982.

34. Kong X, Hellermann GR, Patton G, Kumar M, Behera A, Randall TS, Zhang J, Lockey RF, Mohapatra SS. (2005). An immunocompromised BALB/c mouse model for respiratory syncytial virus infection. Virology Journal 2, 3.

35. Kotani O, Naeem A, Suzuki T, Iwata-Yoshikawa N, Sato Y, Nakajima N, Hosomi T, Tsukagoshi H, Kozawa K, Hasegawa H, Taguchi F, Shimizu H, Nagata N. (2016). Neuropathogenicity of two Saffold virus type 3 isolates in mouse models. PloS One 11, e0148184.

36. Learned LA, Reynolds MG, Wassa DW, Li Y, Olson VA, Karem K, Stempora LL, Braden ZH, Kline R, Likos A, Libama F, Moudzeo H, Bolanda JD, Tarangonia P, Boumandoki P, Formenty P, Harvey JM, Damon IK. (2005). Extended interhuman transmission of monkeypox in a hospital community in the Republic of the Congo, 2003. The American Journal of Tropical Medicine and Hygiene 73, 428~434.

37. Lee PW, Hayes EC, Joklik WK. (1981). Protein sigma 1 is the reovirus cell attachment protein. Virology 108, 156~163.

38. Lorusso A, Teodori L, Leone A, Marcacci M, Mangone I, Orsini M,

Capobianco-Dondona A, Camma C, Monaco F, Savini G. (2015). A new member of the Pteropine orthoreovirus species isolated from fruit bats imported to Italy. Infection, Genetics and Evolution : Journal of Molecular Epidemiology and Evolutionary Genetics in Infectious Diseases 30, 55~58.

39. Maginnis MS, Forrest JC, Kopecky-Bromberg SA, Dickeson SK, Santoro SA, Zutter MM, Nemerow GR, Bergelson JM, Dermody TS. (2006). Beta1 integrin mediates internalization of mammalian reovirus. Journal of Virology 80, 2760~2770.

40. McCormick JB, King IJ, Webb PA, Scribner CL, Craven RB, Johnson KM, Elliott LH, Belmont-Williams R. (1986). Lassa fever. Effective therapy with ribavirin. The New England Journal of Medicine 314, 20~26.

41. Morin MJ, Warner A, Fields BN. (1996). Reovirus infection in rat lungs as a model to study the pathogenesis of viral pneumonia. Journal of Virology 70, 541~548.

42. Nagata N, Iwata N, Hasegawa H, Fukushi S, Harashima A, Sato Y, Saijo M, Taguchi F, Morikawa S, Sata T. (2008). Mouse-passaged severe acute respiratory syndrome-associated coronavirus leads to lethal pulmonary edema and diffuse alveolar damage in adult but not young mice. The American Journal of Pathology 172, 1625~1637.

43. Nibert ML, Odegard AL, Agosto MA, Chandran K, Schiff LA. (2005). Putative autocleavage of reovirus mu1 protein in concert with outer-capsid disassembly and activation for membrane permeabilization. Journal of Molecular Biology 345, 461~474.

44. Odegard AL, Chandran K, Zhang X, Parker JS, Baker TS, Nibert ML. (2004). Putative autocleavage of outer capsid protein micro1, allowing release of myristoylated peptide micro1N during particle uncoating, is critical for cell entry by reovirus. Journal of Virology 78, 8732~8745.

45. Pacitti AF, Gentsch JR. (1987). Inhibition of reovirus type 3 binding to host cells by

sialylated glycoproteins is mediated through the viral attachment protein. Journal of Virology 61, 1407~1415.

46. Parker WB. (2005). Metabolism and antiviral activity of ribavirin. Virus Research 107, 165~171.

47. Paul RW, Lee PW. (1987). Glycophorin is the reovirus receptor on human erythrocytes. Virology 159, 94~101.

48. Plopper CG, Mariassy AT, Wilson DW, Alley JL, Nishio SJ, Nettesheim P. (1983). Comparison of nonciliated tracheal epithelial cells in six mammalian species: ultrastructure and population densities. Experimental Lung Research 5, 281~294.

49. Pourquier P, Gioffre C, Kohlhagen G, Urasaki Y, Goldwasser F, Hertel LW, Yu S, Pon RT, Gmeiner WH, Pommier Y. (2002). Gemcitabine (2',2'-difluoro-2'-deoxycytidine), an antimetabolite that poisons topoisomerase I. Clinical Cancer Research : an Official Journal of the American Association for Cancer Research 8, 2499~2504.

50. Pritchard LI, Chua KB, Cummins D, Hyatt A, Crameri G, Eaton BT, Wang LF. (2006). Pulau virus; a new member of the Nelson Bay orthoreovirus species isolated from fruit bats in Malaysia. Archives of Virology 151, 229~239.

51. Prota AE, Campbell JA, Schelling P, Forrest JC, Watson MJ, Peters TR, Aurrand-Lions M, Imhof BA, Dermody TS, Stehle T. (2003). Crystal structure of human junctional adhesion molecule 1: implications for reovirus binding. Proceedings of the National Academy of Sciences of the United States of America 100, 5366~5371.

52. Ramakrishnan MA. (2016). Determination of 50% endpoint titer using a simple formula. World Journal of Virology 5, 85~86.

53. Rankin JT, Jr., Eppes SB, Antczak JB, Joklik WK. (1989). Studies on the mechanism of the antiviral activity of ribavirin against reovirus. Virology 168, 147~158.

54. Shapouri MR, Kane M, Letarte M, Bergeron J, Arella M, Silim A. (1995). Cloning,

sequencing and expression of the S1 gene of avian reovirus. The Journal of General Virology 76 (Pt 6), 1515~1520.

55. Shimojima M, Fukushi S, Tani H, Yoshikawa T, Fukuma A, Taniguchi S, Suda Y, Maeda K, Takahashi T, Morikawa S, Saijo M. (2014). Effects of ribavirin on severe fever with thrombocytopenia syndrome virus in vitro. Japanese Journal of Infectious Diseases 67, 423~427.

56. Shmulevitz M, Duncan R. (2000). A new class of fusion-associated small transmembrane (FAST) proteins encoded by the non-enveloped fusogenic reoviruses. The EMBO Journal 19, 902~912.

57. Singh H, Shimojima M, Fukushi S, Fukuma A, Tani H, Yoshikawa T, Taniguchi S, Yang M, Sugamata M, Morikawa S, Saijo M. (2016). Serologic assays for the detection and strain identification of Pteropine orthoreovirus. Emerging Microbes & Infections 5, e44.

58. Singh H, Shimojima M, Ngoc TC, Quoc Huy NV, Chuong TX, Le Van A, Saijo M, Yang M, Sugamata M. (2015). Serological evidence of human infection with Pteropine orthoreovirus in Central Vietnam. Journal of Medical Virology 87, 2145~2148.

59. Singh H, Yoshikawa T, Kobayashi T, Fukushi S, Tani H, Taniguchi S, Fukuma A, Yang M, Sugamata M, Shimojima M, Saijo M. (2015). Rapid whole genome sequencing of Miyazaki-Bali/2007 Pteropine orthoreovirus by modified rolling circular amplification with adaptor ligation - next generation sequencing. Scientific Reports 5, 16517.

60. Tan YF, Teng CL, Chua KB, Voon K. (2017). Pteropine orthoreovirus: an important emerging virus causing infectious disease in the tropics? Journal of Infection in Developing Countries 11, 215~219.

61. Tang L, Zhu Q, Qin E, Yu M, Ding Z, Shi H, Cheng X, Wang C, Chang G, Zhu Q, Fang F, Chang H, Li S, Zhang X, Chen X, Yu J, Wang J, Chen Z. (2004). Inactivated SARS-CoV vaccine prepared from whole virus induces a high level of neutralizing

antibodies in BALB/c mice. DNA and Cell Biology 23, 391~394.

62. Tani H, Fukuma A, Fukushi S, Taniguchi S, Yoshikawa T, Iwata-Yoshikawa N, Sato Y, Suzuki T, Nagata N, Hasegawa H, Kawai Y, Uda A, Morikawa S, Shimojima M, Watanabe H, Saijo M. (2016). Efficacy of T-705 (Favipiravir) in the treatment of infections with lethal severe fever with thrombocytopenia syndrome virus. mSphere 1.

63. Taniguchi S, Maeda K, Horimoto T, Masangkay JS, Puentespina R, Jr., Alvarez J, Eres E, Cosico E, Nagata N, Egawa K, Singh H, Fukuma A, Yoshikawa T, Tani H, Fukushi S, Tsuchiaka S, Omatsu T, Mizutani T, Une Y, Yoshikawa Y, Shimojima M, Saijo M, Kyuwa S. (2017). First isolation and characterization of Pteropine orthoreoviruses in fruit bats in the Philippines. Archives of Virology.

64. Thalmann CM, Cummins DM, Yu M, Lunt R, Pritchard LI, Hansson E, Crameri S, Hyatt A, Wang LF. (2010). Broome virus, a new fusogenic orthoreovirus species isolated from an Australian fruit bat. Virology 402, 26~40.

65. Urbano P, Urbano FG. (1994). The reoviridae family. Comparative Immunology, Microbiology and Infectious Diseases 17, 151~161.

66. Voon K, Tan YF, Leong PP, Teng CL, Gunnasekaran R, Ujang K, Chua KB, Wang LF. (2015). Pteropine orthoreovirus infection among out-patients with acute upper respiratory tract infection in Malaysia. Journal of Medical Virology 87, 2149~2153.

67. Weiner HL, Ault KA, Fields BN. (1980). Interaction of reovirus with cell surface receptors. I. Murine and human lymphocytes have a receptor for the hemagglutinin of reovirus type 3. Journal of Immunology (Baltimore, Md : 1950) 124, 2143~2148.

68. Wong AH, Cheng PK, Lai MY, Leung PC, Wong KK, Lee WY, Lim WW. (2012). Virulence potential of fusogenic orthoreoviruses. Emerging Infectious Diseases 18, 944~948.

69. Yamanaka A, Iwakiri A, Yoshikawa T, Sakai K, Singh H, Himeji D, Kikuchi I, Ueda A,

Yamamoto S, Miura M, Shioyama Y, Kawano K, Nagaishi T, Saito M, Minomo M, Iwamoto N, Hidaka Y, Sohma H, Kobayashi T, Kanai Y, Kawagishi T, Nagata N, Fukushi S, Mizutani T, Tani H, Taniguchi S, Fukuma A, Shimojima M, Kurane I, Kageyama T, Odagiri T, Saijo M, Morikawa S. (2014). Imported case of acute respiratory tract infection associated with a member of species Nelson Bay orthoreovirus. PloS One 9, e92777.

70. Yang P, Xing L, Tang C, Jia W, Zhao Z, Liu K, Gao X, Wang X. (2010). Response of BALB/c mice to a monovalent influenza A (H1N1) 2009 split vaccine. Cellular & Molecular Immunology 7, 116~122.
71. Yang ZJ, Wang CY, Lee LH, Chuang KP, Lien YY, Yin HS, Tong DW, Xu XG, Liu HJ. (2010). Development of ELISA kits for antibodies against avian reovirus using the sigmaC and sigmaB proteins expressed in the methyltropic yeast Pichia pastoris. Journal of Virological Methods 163, 169~174.